

University of Texas at Tyler

Scholar Works at UT Tyler

Biotechnology Theses

Biotechnology

2024

Effect of Monoclonal Antibodies MA-33H1F7 and MA-8H9D4 on PAI-1 in Cells Activated with TGF β

Srikar Modukuri

University of Texas at Tyler, smodukuri@patriots.uttyler.edu

Follow this and additional works at: https://scholarworks.uttyler.edu/biotech_grad



Part of the Biotechnology Commons

Recommended Citation

Modukuri, Srikar, "Effect of Monoclonal Antibodies MA-33H1F7 and MA-8H9D4 on PAI-1 in Cells Activated with TGF β " (2024). *Biotechnology Theses*. Paper 20.
<http://hdl.handle.net/10950/4715>

This Thesis is brought to you for free and open access by the Biotechnology at Scholar Works at UT Tyler. It has been accepted for inclusion in Biotechnology Theses by an authorized administrator of Scholar Works at UT Tyler. For more information, please contact tgullings@uttyler.edu.

Effect of Monoclonal Antibodies MA-33H1F7 and MA-8H9D4 on PAI-1 in
Cells Activated with TGF β

By

SRIKAR MODUKURI

A thesis submitted in partial fulfillment of
the requirements for the degree of
Master of Science in Biotechnology
Department of Cellular and Molecular Biology
Andrey A. Komissarov , PhD. Thesis Director
School of Medicine

The University of Texas at Tyler
May 2024

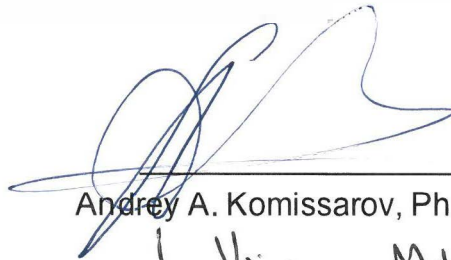
The University of Texas at Tyler
Tyler, Texas

This is to certify that the Master's Thesis of

Srikar Modukuri

has been approved for the thesis requirement on
May 15th, 2024 for
the Master of Science in Biotechnology degree

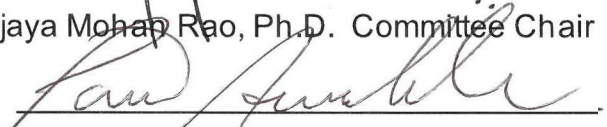
Approvals:



Andrey A. Komissarov, Ph.D. Thesis Director



L. Vijaya Mohan Rao, Ph.D. Committee Chair



Pierre Neuenschwander, Ph.D. Committee Member



Amy Tvinnereim, Ph.D. Committee Member



Ali Azghani, M.D. Committee Member



Mitsuo Ikebe, Ph.D. Chair,
Cellular and Molecular Biology



Brigham Willis, M.D., Dean,
School of Medicine

ABSTRACT

This study investigates the impact of monoclonal antibody treatment on plasminogen activator inhibitor-1 (PAI-1) expression and secretion in transforming growth factor beta (TGF β) activated pleural human mesothelial cells. In this study, we examined total PAI-1 levels in conditioned media from human pleural mesothelial cells under various conditions using immunoblot and enzyme-linked immunosorbent assay techniques (ELISA). Specifically, we targeted PAI-1 with monoclonal antibodies (mAbs) MA-33H1F7 and MA-8H9D4, which bind to unique epitopes on PAI-1. A reduction in PAI-1 levels was observed between control and antibody-treated cells by immunoblot analysis of cell conditioned media. ELISA results also revealed a reduction in total PAI-1 levels in the conditioned media of cells treated with antibodies. A decrease of 30-50% was observed upon addition of 50 $\mu\text{g}/\text{mL}$ MA-33H1F7 and 50 $\mu\text{g}/\text{mL}$ MA-8H9D4 of each antibody, with a similar reduction at 100 $\mu\text{g}/\text{mL}$ concentration. Immunofluorescence (IFC) results corroborated the findings of the ELISA and Immunoblot, but quantification of the PAI-1 detected in IFC demonstrated a lack of statistical significance. This research underscores the complexity of PAI-1 regulation and highlights the need for further elucidation of the effects of antibody targeting on PAI-1 expression in TGF β activated cells.

TABLE OF CONTENTS

ABSTRACT	iii
TABLE OF CONTENTS	iv
LIST OF FIGURES.....	vi
LIST OF TABLES.....	vii
LIST OF ABBREVIATIONS.....	viii
INTRODUCTION.....	1
Empyema and Intrapleural Fibrinolytic Therapy	1
PAI-1 Targeting.....	2
RESEARCH HYPOTHESIS	7
MATERIALS AND METHODS	8
Cell Culture	8
Immunoblot Analysis.....	9
Enzyme-Linked Immunosorbent Assay (ELISA).....	10
Immunofluorescence	11
Statistical Analysis	13
RESULTS.....	15
Effect of Antibody Treatment on PAI-1 Levels.....	15
ELISA: Changes in PAI-1 Levels in Response to Antibody Treatment.....	33
Relationship Between Immunoblot Data and ELISA Data.....	35
Analysis of PAI-1 in Cell Lysates	39
Immunofluorescence	42
DISCUSSION.....	48
Introduction to the Study.....	48
Immunoblot Results Indicate PAI-1 Levels Are Reduced in CM of Activated Cells Treated With mAbs	49
ELISA Data Supports The Immunoblot Data	52
Immunoblot of Cell Lysates Was Inconclusive	56

IFC Indicates mAbs Reduce PAI-1 Levels in Cells.....	58
CM and Cell Analysis Indicates mAbs Reduce PAI-1 Levels	61
Possible Mechanisms of Reduction in PAI-1 Due to mAbs	62
Proteolysis and PAI-1	63
Signaling Pathways and mAbs	63
Conclusions and Future Steps.....	64
REFERENCES.....	67
VITA	70

LIST OF FIGURES

Figure 1: mAbs mediated PAI-1 Neutralization Targeting Mechanism.	4
Figure 2: Schematic representation of the experimental treatment protocol for cell trials.....	17
Figure 3: Immunoblot of PAI-1 in CM and GAPDH in Cell Lysate.	19
Figure 4: Additional Bands Observed at 100KDa.	20
Figure 5: Reduction of PAI-1 Due to mAbs Treatment in Activated Cells.	22
Figure 6: Densitometry of PAI-1 Immunoblot Data Showing Relative Band Density.	25
Figure 7: ELISA Standard Curves.....	28
Figure 8: PAI-1 ELISA Data from the R&D Systems Kit.	31
Figure 9: ELISA data Shows a Reduction in PAI-1 Levels in mAbs Treated Sample.	34
Figure 10: Comparison of PAI-1 levels from Immunoblots and ELISAs.	36
Figure 11: Correlation Plot of PAI-1 Immunoblots Versus ELISAs.	38
Figure 12: Detection of PAI-1 in Cell Lysates.	41
Figure 13: Immunohistochemistry Analysis of PAI-1 Levels in Human Mesothelial Cells.	43
Figure 14: PAI-1 Intensity via Immuno-Fluorescence.	44
Figure 15: IFC Analysis of PAI-1 in Human Mesothelial Cells.	46
Figure 16: IFC Data for PAI-1 with mAbs Treatment.	47

LIST OF TABLES

Table 1: Table of PAI-1 Concentrations from Conditioned Media.....	33
--	----

LIST OF ABBREVIATIONS

BCA: Bicinchoninic Acid Assay

CL: Cell Lysate

CM: Conditioned Media

DAPI: 4',6-diamidino-2-phenylindole

DPBS: Dulbecco's Phosphate-Buffered Saline

ELISA: Enzyme-Linked Immunosorbent Assay

FBS: Fetal Bovine Serum

GAPDH: Glyceraldehyde 3-phosphate dehydrogenase

GFP: Green Fluorescent Protein

HRP: Horseradish Peroxidase

IPFT: Intrapleural Fibrinolytic Therapy

mAb: Monoclonal Antibodies

MI: Molecular Innovations™

PAI-1: Plasminogen Activator Inhibitor-1

PBS: Phosphate Buffered Saline

PBST: Phosphate Buffered Saline with Tween™

qPCR: Quantitative Polymerase Chain Reaction

PVDF: Polyvinylidene Fluoride

R&D: R&D Systems™

RIPA: Radioimmunoprecipitation Assay Buffer

RPMI: Roswell Park Memorial Institute (media)

TBS-T: Tris-buffered saline with Tween

TGF β : Transforming Growth Factor Beta

TMB: 3,3',5,5'-Tetramethylbenzidine

tPA: Tissue-Type Plasminogen Activator

uPA: Urokinase-Type Plasminogen Activator

INTRODUCTION

Empyema and Intrapleural Fibrinolytic Therapy

Empyema, a debilitating condition characterized by the accumulation of pus in the pleural cavity, presents formidable challenges in clinical management and treatment [1]. Empyema progresses through three distinct stages, the exudative, fibrinopurulent, and organizing. Each stage entails unique pathophysiological changes which impact how the empyema is treated [2]. The exudative stage is characterized by the increase in fluid in the pleural space due to elevated capillary permeability, resulting from high level of proinflammatory cytokines. The fibrinopurulent stage, marked by the accumulation of fibrin clots and membranes within the pleural space, leads to impaired lung function and the formation of loculated pleural effusions [3]. Finally, the organizing is characterized by the formation of a dense fibrin mesh that encapsulates the lung, resulting in restrictive respiratory dysfunction [4].

Traditional treatments for empyema, including surgical interventions aimed at removing fibrin clots and membranes, pose significant risks, particularly in elderly patients who constitute a considerable portion of empyema cases. The increased surgical risk in elderly patients underscores the importance of exploring alternative therapeutic approaches.

Intrapleural fibrinolytic therapy (IPFT), although involving surgery, offers a less invasive therapeutic option for late-stage empyema compared to traditional

surgical interventions. By administering fibrinolytic agents directly into the pleural space, IPFT aims to dissolve fibrin clots and facilitate drainage, thereby alleviating respiratory compromise and improving clinical outcomes [5]. IPFT offers several advantages over traditional surgical treatment including lower risk of complications, and potentially shorter hospital stays.

Plasminogen activator inhibitor-1 (PAI-1), a key regulator of fibrinolysis, has garnered significant attention in the context of empyema pathogenesis and treatment. Elevated levels of PAI-1 are associated with poor treatment outcomes in empyema patients, and PAI-1 has been found to be overexpressed in the pleural fluids in empyema by up to three orders of magnitude [6]. This suggests that the inhibition of PAI-1 can improve the efficacy of IPFT.

PAI-1 Targeting

Previous research has demonstrated the potential of PAI-1 targeting to enhance the efficacy of IPFT in animal models of empyema [7-9]. Studies utilizing mAbs and a small docking site peptide have yielded promising outcomes, including a significant reduction in the minimal effective dose of IPFT [7]. The minimal effective dose is defined as the dose of plasminogen activator which produces effective treatment for every animal within the treatment group [7]. Specifically, PAI-1 targeting reduced the minimal effective dose of IPFT by 8 times in tetracycline-induced empyema models, 8 times in infectious acute empyema

models, and at least 4 times in infectious chronic empyema rabbit models [8, 9]. The discrepancy in effectiveness observed between acute and chronic empyema models following PAI-1 targeting prompts an investigation into potential cellular responses influencing treatment outcomes.

This study aims to address this gap in knowledge by investigating the effects of PAI-1 targeting with mAbs on activated human pleural mesothelial cells. By focusing on human mesothelial cells, we intend to establish a cellular model to scrutinize the impact of PAI-1 targeting on PAI-1 levels produced by the cells. Understanding how human mesothelial cells respond to PAI-1-targeted therapies could illuminate underlying mechanisms contributing to the reduced effectiveness observed in chronic empyema models. By utilizing mAbs MA-33H1F7 and MA-8H9D4, known for their high specificity and affinity to human PAI-1, we seek to elucidate the influence of these antibodies on PAI-1 expression and/or secretion in human mesothelial cells [10].

PAI-1 reacts with target proteins such as tissue plasminogen activator (tPA) or urokinase plasminogen activator (uPA) through the inhibitory pathway seen in Figure 1. Both antibodies inhibit PAI-1 activity through redirection of the enzymatic pathway of PAI-1 to the substrate branch, seen in Figure 1, in which the reactive center loop is inserted the β -Sheet A of the PAI-1 molecule [11]. Ma-33H1F7 binds to an epitope at α -Helix F, observed in cyan in Figure 1, and MA-8H9D4 binds to an epitope on the end opposite of the reactive center loop of PAI-1, indicated as

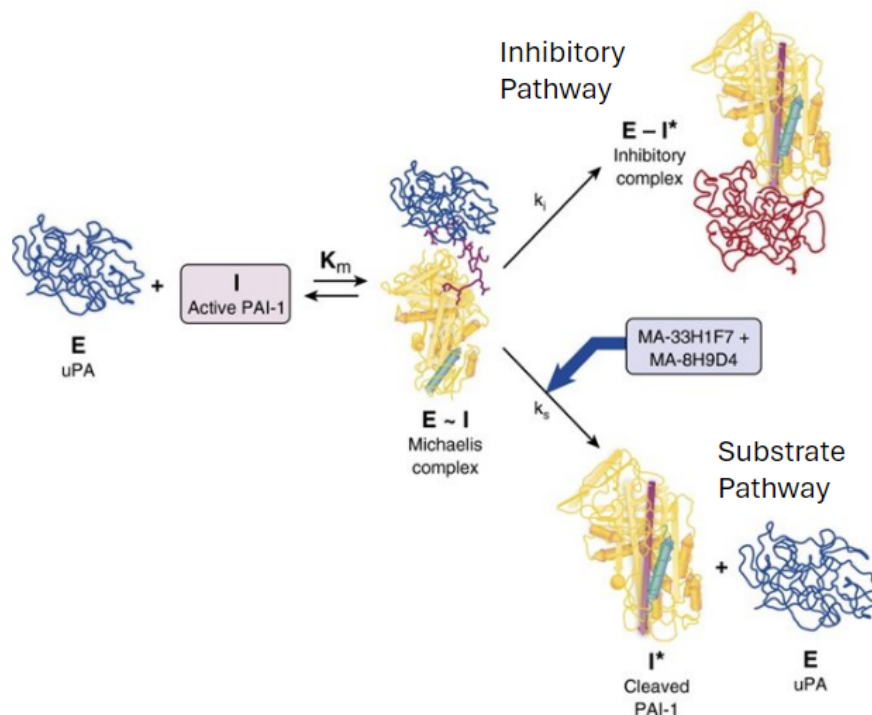


Figure 1: mAb mediated PAI-1 Neutralization Targeting Mechanism. Schematic representation of the mechanism by which mAbs MA-33H1F7 and MA-8H9D4 interact with plasminogen activator inhibitor 1 (PAI-1), leading to the redirection of the PAI-1 mechanism to its substrate branch and resulting in inactive, cleaved PAI-1. Published by Florova, G., et al. 2015.

the bottom of PAI-1 in the scheme. Both antibodies can bind to an individual PAI-1 molecule at once, due to the two different epitopes.

Detection of PAI-1 expression and secretion in cell samples typically relies on two main methodologies: Immunoblot analysis and enzyme-linked immunoassay (ELISA). Immunoblotting allows for the detection of various forms of PAI-1, including complexed, latent, active, and cleaved forms, through the use of specific primary antibodies that recognize PAI-1 epitopes. Figure 1 shows Michaelis complex (E~I) and cleaved (I*) PAI-1 and it can be seen that cleaved PAI-1 results in an insertion of the reactive center loop, seen in red. Latent PAI-1 is formed spontaneously and results in a PAI-1 with an inserted reactive center

loop [12]. Complexed PAI-1 appears as additional bands under denaturing conditions on an Immunoblot assuming that the PAI-1 is covalently bound in the complex, as uPA is seen bound in the inhibitory complex, E~I*, in Figure 1 [13]. Latent and active PAI-1 the same molecular weight (45kDa) and will be observed as a single band. Cleaved PAI-1 will appear as a slightly lower band (41kDa) compared to active/latent. A Immunoblot will not reveal degraded PAI-1 as primary antibodies will not readily bind to degraded PAI-1. Conversely, ELISA enables the quantification of total PAI-1 antigen levels, including complexed, latent, active, and cleaved PAI-1, using specific capture and detection antibodies that bind to PAI-1. This means that an ELISA result will reflect detection of all PAI-1 in the sample, including PAI-1 bound in an inhibitory complex (E~I). In order to provide additional validation, this study utilized immunofluorescence (IFC). IFC is based in a similar methodology to Immunoblotting, through IFC allows for detection of the protein of interest, PAI-1, directly on the cell surface. A primary antibody is applied directly to the target cells, which binds PAI-1 on the cell surface. A fluorescent secondary antibody is utilized and imaged under a confocal microscope, allowing for the visualization of PAI-1 directly on the cells.

Through a comprehensive analysis combining Immunoblot, ELISA, and IFC methodologies, we aim to characterize the changes in PAI-1 levels induced by antibody treatment and establish a methodology by which the effects of PAI-1 targeting can be analyzed on a cellular level. Transitioning from rabbit models of PAI-1 targeting to cellular investigations, this study aims to demonstrate cellular

responses to PAI-1 targeting, offering a pathway for pioneering therapeutic strategies to enhance treatment outcomes for patients with chronic empyema.

RESEARCH HYPOTHESIS

The treatment of transforming growth factor beta activated mesothelial cells with mAbs MA-33H1F7 and MA-8H9D4 antibodies will lead to a reduction in PAI-1 expression/secretion compared to untreated cells. Furthermore, excess antibody concentration may result in a further augmentation of PAI-1 levels. The Specific Aims of the study are to:

1. Establish a methodology to analyze the effects of PAI-1 targeting on human mesothelial cells.
2. Determine if mAbs treatment of activated human mesothelial cells will result in a reduction in PAI-1 levels detected in conditioned media and within the cells.

MATERIALS AND METHODS

Cell Culture

Human mesothelial cells (Met5A) were cultured in RPMI growth media supplemented with 10% fetal bovine serum (FBS) and 1% penicillin-streptomycin. Cells were maintained in a humidified incubator at 37°C with 5% CO₂.

Prior to treatment, cells were serum-starved for 3-5 hours to synchronize growth and minimize serum-related effects. Following serum starvation, cells were treated with TGFβ at a concentration of 10 ng/mL to induce activation. In experimental samples, mouse IgG1 mAbs MA-33H1F7 and MA-8H9D4 were added (50μg/mL and 100μg/mL each) alongside the TGFβ treatment. Both antibodies are used in conjunction in equal concentrations for experimental groups containing mAbs treatment. Antibodies obtained from Paul Declerck, PhD, Dean at the Faculty of Pharmaceutical Sciences at the University of Leuven, Belgium.

Cell confluency was visually monitored under a microscope to ensure uniform growth and treatment conditions. Cells were seeded into appropriate culture vessels at a predetermined density to ensure proper attachment and growth. TGFβ was pipetted into the culture media to achieve the desired concentration, and cells were allowed to incubate for a specified period. After incubation, both adherent cells and cell culture supernatants were collected for further analysis.

Immunoblot Analysis

Cell lysates were prepared from cell samples using radioimmunoprecipitation assay (RIPA) buffer supplemented with protease inhibitors. Total protein concentration was determined using the Bicinchoninic Acid Assay (BCA). Equal amounts of protein (50 µg) were loaded onto a Invitrogen™ NuPAGE™ 12%, Bis-Tris, 1.0 mm, Protein Gel and electrophoresed at 80-100V for 0.5 hours, followed by 100-120V for 1-2 hours until adequate separation was achieved.

Proteins were transferred onto polyvinylidene difluoride (PVDF) membranes using a semi-dry transfer system at 150V for 1 hour. Membranes were activated with methanol and assembled in a sandwich configuration with filter paper and sponges soaked in transfer buffer for 2-5 minutes. After transfer, membranes were blocked with 5% non-fat milk in Tris-buffered saline with Tween 20 (TBS-T) for 1 hour at room temperature.

Membranes were incubated with rabbit polyclonal primary antibody against human PAI-1 (ab66705, 0.2µg/mL, Abcam™), and mouse monoclonal anti-human PAI-1 (sc-5297, 0.2µg/mL, Santa Cruz Biotechnology, INC.) overnight at 4°C. After washing with TBS-T, membranes were incubated with appropriate secondary antibodies: horseradish peroxidase (HRP)-conjugated donkey anti-rabbit IgG (711-035-152, Jackson ImmunoResearch Laboratories, INC) for rabbit primary antibody and HRP-conjugated donkey anti-mouse IgG (AffiniPure Peroxidase Conjugated Donkey Anti-Mouse IgG, Jackson ImmunoResearch Laboratories,

INC) for mouse primary antibody, both at a concentration of 0.08µg/mL. Protein bands were visualized using SuperSignal West Femto Maximum Sensitivity Substrate (Thermo Fisher Scientific) and imaged with a chemiluminescence imaging system (ChemiDoc Imaging System, Bio-Rad). Glyceraldehyde 3-phosphate dehydrogenase, (GAPDH) was used as a loading control for lysate samples and detected with anti-GAPDH antibody mouse monoclonal primary (GA1R, ab125247, Abcam™) with donkey anti-mouse secondary (AffiniPure Peroxidase Conjugated Donkey Anti-Mouse IgG, Jackson ImmunoResearch Laboratories, INC) (0.08µg/mL). Band intensities were quantified using ImageJ densitometry analysis software.

Enzyme-Linked Immunosorbent Assay (ELISA)

The concentration of PAI-1 in the cell culture supernatants was determined using ELISA kits from R&D Systems (Catalog #: DTSE100), and Molecular Innovations (Catalog # HPAIKT-TOT). The specific antibodies used by the kits could not be identified as it is confidential information, however the clonality of the antibodies was listed. The R&D systems kit utilizes a polyclonal capture antibody specific for PAI-1 and an enzyme-linked polyclonal primary antibody specific for human total PAI-1. The Molecular Innovations kit utilized a monoclonal capture antibody and a polyclonal anti-human primary. Both kits followed a similar standardized procedure, with addition of samples on pre-coated plates, addition of

primary, secondary, and then substrate. For the R&D Systems kit, 96-well plates were coated with a monoclonal capture antibody provided in the kit. After blocking with assay buffer, samples, diluted at 1:5 ratio with assay diluent, were added to the wells in duplicate and incubated for 2 hours. The plates were then washed, and detection antibody was added, followed by incubation with HRP-conjugated streptavidin. After washing, the plates were developed with tetramethylbenzidine (TMB) substrate solution, and the reaction was stopped with 1N sulfuric acid. Absorbance was measured at 450 nm using a Synergy H1 Hybrid Microplate Reader. A standard curve was generated using known concentrations of recombinant PAI-1 provided in the kit. The MI standards ranged from 100ng/mL PAI-1 to 0.25ng/mL PAI-1. The R&D standards ranged from 20ng/mL to 0.313ng/mL. A second standard curve was generated as a duplicate of the first with 50µg/mL each of MA-33H1F7 and MA-8H9D4 added to each well. The Molecular Innovations (Catalog # HPAIKT-TOT) kit was used similarly, with minor modifications in the assay protocol to confirm antibody interference of PAI-1 signal detection.

Immunofluorescence

IFC was utilized in order to visualize PAI-1 directly on the Met5A cells. For the IFC procedure, Met5A cell samples were plated in T25 flasks and allowed to incubate overnight. Once adhered, the cells were washed with 1x Dulbecco's

Phosphate-Buffered Saline (DPBS) and maintained in Roswell Park Memorial Institute Medium (RPMI). Upon reaching 50-90% confluence, the cells were seeded to an 8-well chambered slide for immunofluorescence analysis.

After 18 hours of incubation at 37°C, the cells were then starved with serum free-media, same as in the initial cell culture steps, for 3-5 hours. Following starvation certain wells were treated with 10ng/mL TGFβ. In the experimental group, antibodies MA-33H1F7 and MA-8H9D4 were added (50µg/mL and 100µg/mL each) alongside the TGFβ treatment. A control was made which lacked TGFβ treatment, and another control was made which contained mAbs, 50µg/mL each, but no TGFβ. The cells were left to incubate overnight with the treatment.

Following overnight incubation, the cells were washed 3 times with DPBS. The cells were fixed and permeabilized through incubation in 100% methanol (chilled at -20°C) for 10 minutes. After fixation, the cells were washed three times with ice-cold PBS.

Following washing, the cells were blocked to prevent nonspecific antibody binding by incubating with 2% horse serum in PBST (PBS with 0.1% Tween 20) for 1 hour. Subsequently, the cells were incubated with primary antibodies diluted in 1% horse serum in PBST, including rabbit monoclonal anti-human PAI-1 (ab307393, Abcam™, 0.1µg/mL). The primary incubation was conducted overnight at 4°C.

After primary antibody incubation, the cells were washed three times with PBST and then incubated with secondary antibodies diluted in 1% horse serum for

1 hour at room temperature. The secondary antibodies used was Alexa Fluor 488 Goat anti-rabbit (ab150077, Abcam™, 0.1µg/mL) for PAI-1. Hoechst 33342 nuclear stain (Invitrogen, 0.1µg/mL) was added alongside the PAI-1 secondary antibody. Following secondary antibody incubation, the cells were washed three times with PBS to remove unbound antibodies. Finally, the cells were mounted with a drop of mounting medium (Fluoromount-G™), and a coverslip was placed over the sample. The coverslip was sealed with nail polish to prevent dehydration, and the slides were stored at -20°C until imaging.

Cellular imaging was performed using a Cytation 10 confocal microscope, capturing images in the DAPI (for nuclear staining, 405nm) and GFP (for PAI-1, 488nm) channels. This allowed for the visualization and analysis of PAI-1 directly within the cells. Image analysis and statistical analysis was performed utilizing BioTek Gen5 Software.

Statistical Analysis

Data obtained from Immunoblot and ELISA experiments were analyzed using GraphPad Prism™ version 9.0.0 (GraphPad Software). For Immunoblot analysis, band densities were quantified using ImageJ software (National Institutes of Health). Correlation analysis was performed utilizing GraphPad Prism, with a significant positive correlation indicated by (≥ 0.7), moderate correlation by (> 0.5) and low correlation by (> 0.2). Statistical significance between experimental groups

was determined using one-way analysis of variance (ANOVA) followed by Tukey's post-hoc test for multiple comparisons. A p -value less than 0.05 was considered statistically significant. For ELISA data, standard curves were generated using a four-parameter logistic curve fit model, and PAI-1 concentrations were calculated based on the absorbance readings of sample wells. Statistical significance between groups was assessed using one-way ANOVA followed by Tukey's post-hoc test. All statistical tests were two-sided, and a p -value less than 0.05 was considered statistically significant. IFC results were analyzed through Biotech™ Gen5 (3.15.15) data collection and analysis software.

RESULTS

Effect of Antibody Treatment on PAI-1 Levels

In order to understand the effects of MA-33H1F7 and MA-8H9D4 on PAI-1 expression in Met5A cells, we devised a cell treatment scheme which would allow for the treatment of cells with TGF β , to activate the cells, and treatment with the mAbs, targeting PAI-1. Figure 2 displays the schematic representation of the cell treatment scheme which was used in the previous stage of the study. In this study MA-33H1F7 and MA-8H9D4 were only used in concert, and therefore "mAb" in Figure 2 refers to both antibodies in equal concentration (50 μ g/mL or 100 μ g/mL). Furthermore, the concentrations of mAbs used is directly reflective of the level of mAbs used in the treatment of Tetracycline induced pleural injury in the prior study, which equates to approximately 80 μ g/mL [7]. The dissociation constant for both MA-33H1F7 and MA-8H9D4 are both in the nanomolar range [14]. Therefore, both 50 μ g/mL (0.333 μ M) mAbs and 100 μ g/mL (0.533 μ M) mAbs treatment will result in an excess of mAbs in relation to PAI-1. Utilization of both the low and high range of mAbs treatment allows for the determination if the effect of mAbs is solely on PAI-1 or if excess mAbs treatment results in further changes in PAI-1 levels. In subsequent sections of the results, "mAbs" refers to the combined use of MA-33H1F7 and MA-8H9D4 antibodies in equal concentration unless otherwise specified.

The experimental conditions utilized in our cell treatment scheme encompassed:

- Control (–TGF β , –mAbs): Met5A cells incubated, post-starvation, without TGF β stimulation or mAbs treatment served to establish baseline PAI-1 expression levels.
- TGF β Activation (+TGF β 10ng/mL, –mAbs): Met5A cells incubated, post-starvation, with TGF β stimulation to induce PAI-1 expression in the absence of mAbs intervention represented the TGF β activation group, which establishes a baseline for PAI-1 expression in activated cells.
- TGF β Activation with mAbs Treatment (+TGF β 10ng/mL, +mAbs 50 μ g/mL and 100 μ g/mL): Met5A cells incubated, post-starvation, with both TGF β and mAbs. The use of two concentrations of antibody treatment allowed for the determination of the effect of increasing antibody concentration on PAI-1 expression and secretion.

Nine replicate cell trials were performed and labeled (trial 1, trial 2...). Each cell trial had a negative and positive TGF β control as well as samples treated with mAbs MA-33H1F7 and MA-8H9D4, in equal concentrations, as demonstrated in Figure 2.

This study proceeded in 2 stages. The main stage of this study aimed to identify and quantify PAI-1 levels in the conditioned media (CM), obtained from the cell

trials. The second stage involved the analysis of PAI-1 within the cells themselves, involving detection of PAI-1 in cell lysates as well as the utilization of IFC.

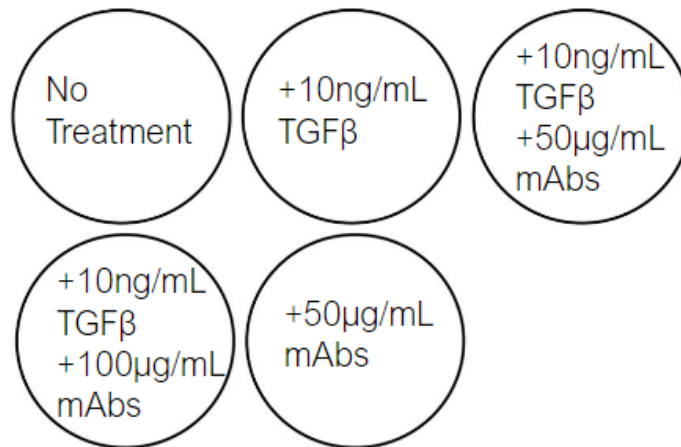


Figure 2: Schematic representation of the experimental treatment protocol for cell trials. A total of nine trials were made, each using the same treatment scheme. Cells were treated with TGFβ alone or in combination with mAbs MA-33H1F7 and MA-8H9D4, targeting PAI-1. Treatment conditions were identical across trials, $n=9$.

Following retrieval of cell CM and lysates, the Immunoblotting procedure was carried out in order to determine the effect of the antibody treatment on PAI-1 levels. Cell lysates were also analyzed for GAPDH for the purposes of normalization.

Figure 3A depicts the presence of PAI-1 bands in conditioned media samples loaded on NuPAGE gels and probed for PAI-1 using mouse anti-human (trials: 1-5) PAI-1 or rabbit anti-human PAI-1 antibodies (trials: 7-9). Lysates were probed with anti-GAPDH antibody in order to normalize the Immunoblot data from the CM samples and can be seen in Figure 3B. Immunoblots of cell sample and conditioned media from trials 4 and 6 could not be resolved and bands were faint

or entirely absent on membrane, and so these trials are not present in immunoblot analysis.

As seen in Figure 3, there was variation in band patterns between cell trials. Specifically, 3 trends can be observed. Firstly, in trials 1 and 2, there appears to be a reduction in PAI-1 band intensity in samples treated with both mAbs and TGF β , compared to the TGF β control. Secondly, there appeared to be no discernable differences between PAI-1 levels in the CM for trials 3 and 5. Thirdly, trials 7, 8, and 9 yielded Immunoblots which appeared to show an increase in PAI-1 according to the antibody treatment in TGF β activated samples. In each of these Immunoblots, additional bands was observed between 100kDa and 75kDa as seen in Figure 3. As prior research and established literature has shown [15], it is expected that PAI-1 levels are to significantly increase in Met5A cells treated with TGF β . Immunoblot results of trials 3 and 5, which displayed no major increase in PAI-1 band intensity due to TGF β treatment were excluded from further analysis. Cell trials 1, 2, 7, 8, and 9 all contained a positive control (+TGF β) PAI- band which had higher band intensity than the negative control (-TGF β). This indicates that these trials possessed controls which are in line with published data, and therefore were the focus of following analysis.

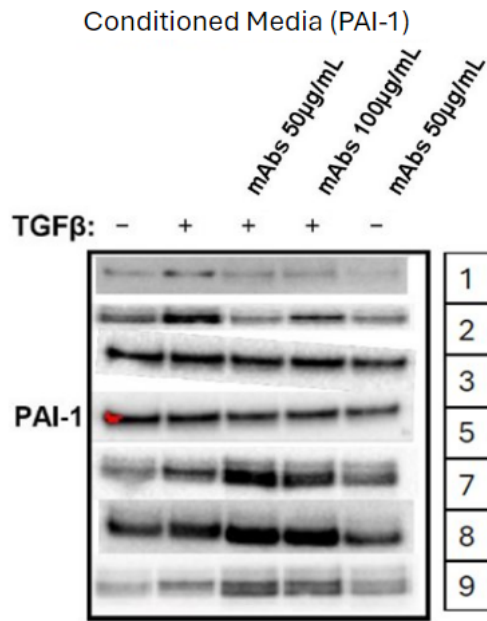
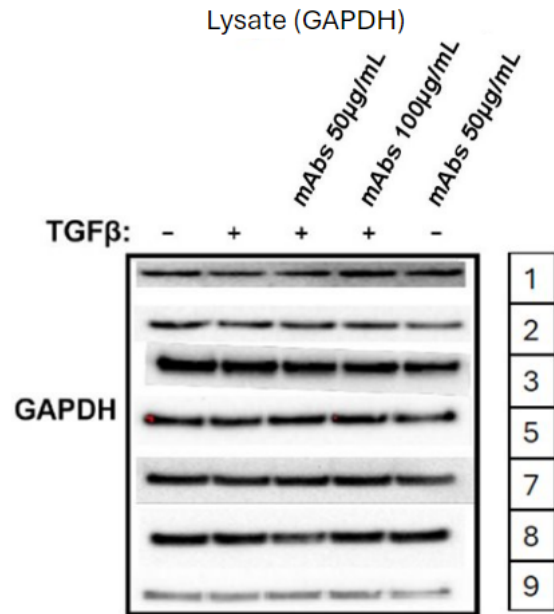
A.**B.**

Figure 3: Immunoblot of PAI-1 in CM and GAPDH in Cell Lysate.

Immunoblot bands showing the expression of plasminogen activator inhibitor-1 (PAI-1) in conditioned media (Panel A) and corresponding GAPDH bands from cell lysate (Panel B) across seven cell trials. Conditioned media was collected and subjected to Immunoblot analysis using antibodies against PAI-1. Cell lysates were collected and probed for GAPDH as a control. Membrane was probed for PAI-1 antigen using the primary antibody rabbit anti-human PAI-1 (0.2µg/mL) followed by secondary antibody goat anti-rabbit IgG (0.8µg/mL) (trials: 7,8,9). For trials 1-5, the membrane was probed for PAI-1 antigen using the primary antibody mouse anti-human PAI-1 (ab66705) (0.2µg/mL) followed by secondary antibody AffiniPure Donkey Anti-Mouse IgG (dilution 0.08µg/mL). GAPDH (primary: anti-GAPDH antibody GA1R) was used as for lysate samples and utilized donkey anti-mouse secondary (0.08µg/mL). Bands visualized at 48kDa was assumed to be the expected PAI-1 band and is seen in 3A. The bands were visualized using chemiluminescent detection, and the intensities were quantified to assess PAI-1 levels.

Figure 4 shows the Immunoblot result of cell trial 9, which contained similar bands for both PAI-1 and additional bands of the Immunoblot results of n=3 trials. PAI-1 antigen is detected using rabbit anti-PAI-1 antibody followed by goat anti-rabbit secondary antibody. The PAI-1 band, at 47kDa, in this gel is seen as an upper and lower band. The intensity of the lower band increases in lanes treated

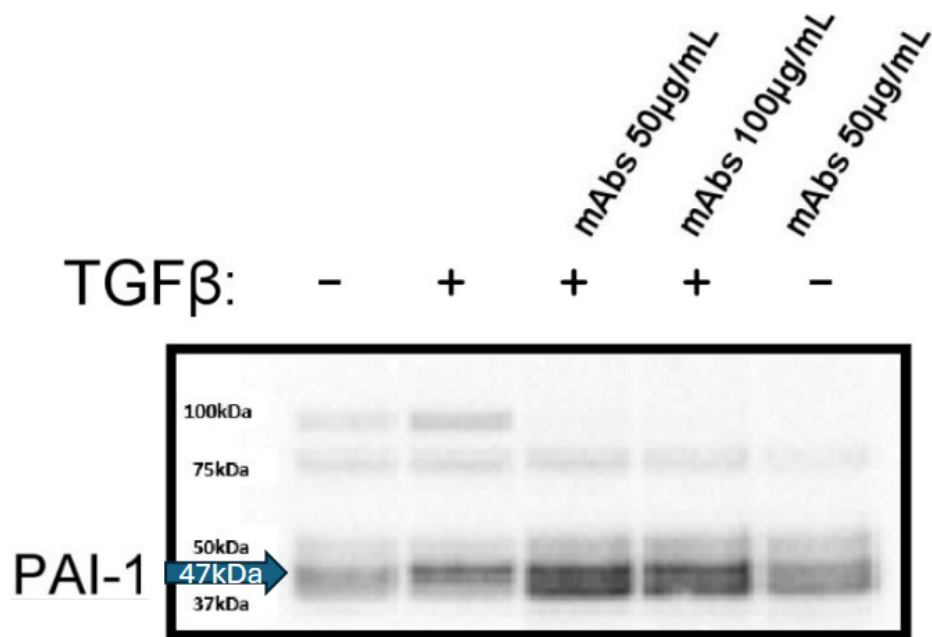


Figure 4: Additional Bands Observed at 100KDa. Conditioned media samples were loaded onto a non-reducing gel. The gel was ran and proteins transferred to a PVDF membrane. Membrane was probed for PAI-1 antigen using the primary antibody rabbit anti-human PAI-1, ab66705, (0.5µg/mL) followed by secondary antibody goat anti-rabbit IgG (0.8µg/mL). Nova 4X Ladder was used to determine molecular weight of detected bands (marked with molecular weight in kDa). Blue arrow indicates PAI-1 band at 47kDa. Number of replicates: $n = 3$.

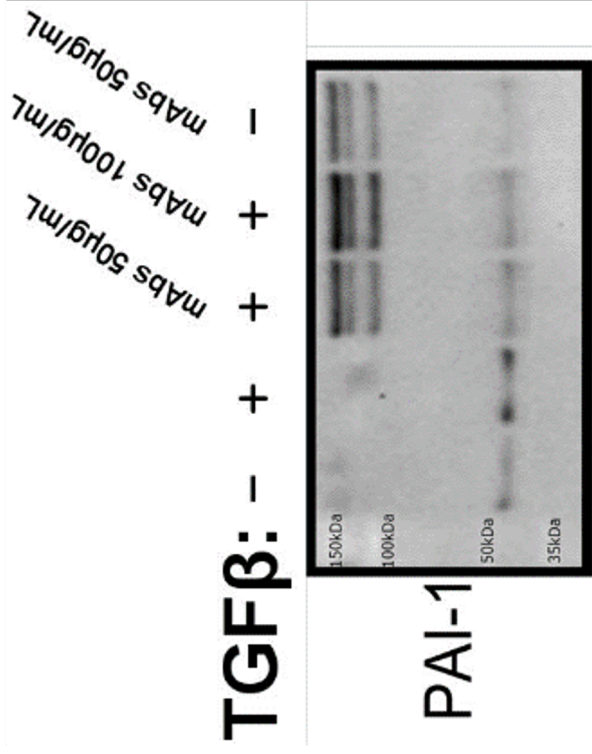
with both MA-33H1F7 and MA-8H9D4. The TGFβ control shows a thinner, more concentrated PAI-1 band than the other samples. Overall, the PAI-1 band appears to increase in intensity in lanes containing sample treated with TGFβ and mAbs. Additionally, 2 bands are observed above the PAI-1 band in the first two lanes, one

at 100kDa and the other around 75kDa. The upper band (100kDa) is not visible in the last 3 lanes. Accumulation of cleaved PAI-1 and the disappearance of the 100kDa band in the presence of mAbs (Fig 4, seen in lanes 3-5) may reflect the mechanism of PAI-1 neutralization. The other two trials which exhibited these additional bands did not have clear separation of the PAI-1 band, as seen in Figure 3. Instead, the PAI-1 band was seen as one large band, which grows darker in the +TGF β +mAbs conditions (refer to Figure 3A).

Figure 5A shows the Immunoblot results of the CM from cell trial 1 probed for PAI-1. The bands were visualized using a mouse anti-PAI-1 monoclonal antibody (C-9), which detects total PAI-1. An anti-mouse secondary was used for this Immunoblot. The blot appears to show a decrease in the PAI-1 band intensity in the lanes corresponding to sample treated with both TGF β and PAI-1 targeting antibodies. Additionally, the Immunoblot demonstrates bands in antibody treated lanes at around 150 kilodaltons to around 100kDa. These bands appear darker in the 100 μ g/mL antibody lane than the 50 μ g/mL antibody lanes.

It was hypothesized that these additional bands were indicative of the secondary antibody, used for detection (anti-mouse), was detecting the mouse origin mAbs utilized for treatment. Figure 5B reflects the results of a control immunoblot performed with mAbs added. Lane 1 contains only loading dye, lane 2 contains 50 μ g/mL IgG antibody, lane 3 contains 50 μ g/mL mAbs, lane 4 contains 100 μ g/mL mAbs, and lane 5 also contains 50 μ g/mL mAbs. The PVDF membrane was probed only with the same anti-mouse secondary utilized for Figure 5A; no

A.



B.

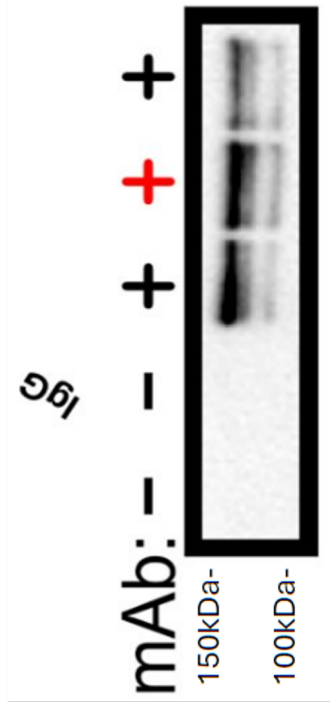


Figure 5: Reduction of PAI-1 Due to mAb Treatment in Activated Cells.

Panel A: An immunoblot of conditioned media sample (trial 1) loaded onto nuPAGE gel, separated by electrophoresis, and transferred to PVDF membranes. The membrane was probed for PAI-1 antigen using the primary antibody mouse anti-human PAI-1 (C-9) (0.5µg/mL), followed by secondary antibody AffiniPure Donkey Anti-Mouse IgG (0.8µg/mL). 4X Nova Ladder present in leftmost lane, marked with MW values in kDa.. Protein bands were visualized using SuperSignal West Femto Maximum Sensitivity Substrate. GAPDH was as a loading control. Number of replicates: n = 4.

Panel B: Immunoblot image of mAb treated samples loaded onto gel alongside an IgG control (IgG:50µg/mL, mAb:50µg/mL). IgG and mAbs were loaded onto nuPAGE gel, separated by electrophoresis, and transferred to PVDF membranes. Lane 1 contains only loading dye, lane 2 contains 50µg/mL IgG antibody, lane 3 contains 50µg/mL mAbs, lane 4 contains 100µg/mL mAbs, and lane 5 also contains 50µg/mL mAbs. Membrane was probed for secondary antibody AffiniPure Donkey Anti-Mouse IgG (0.08µg/mL) and visualized using chemiluminescent substrate. Red + indicates double concentration of mAbs (100µg/mL).

primary was used. Detection with chemiluminescent substrate revealed bands at 150kDa present only in lanes 3, 4, and 5 of Figure 5A. No bands at this molecular weight was present in other lanes. The bands in lane 4 were clearly darker than that seen in lanes 5 and 3, supporting the hypothesis that the 150kDa band is indicative of cross reactivity with the immunoblot secondary antibody and the mAbs used for cell treatment.

Following the acquisition of Immunoblot images for each cell trial, our investigation progressed to a quantitative phase aimed at analyzing the changes PAI-1 levels between experimental conditions. In order to quantify the CM Immunoblot data and detect more minor differences in band density, densitometry analysis was performed for each Immunoblot of CM. The bands identified as PAI-1, at 47kDa, were measured and normalized with the GAPDH bands obtained from the lysate Immunoblots. Normalization was performed by densitometry analysis of the PAI-1 bands and densitometry analysis of the GAPDH bands by calculating the density of the target protein in each lane and multiplying that with the ratio of the highest density GAPDH band to the density of GAPDH bands in the individual lanes. Fold difference was then calculated by determining the ratio of the normalized density per each lane to the normalized density of the +TGF β control. Trials 1, 2, 7, 8, and 9 were utilized for the densitometry analysis as these trials possessed PAI-1 band pattern of the controls which lines up with prior studies and accepted literature.

Densitometry analysis of the Immunoblot data is shown in Figure 6 as the average of the fold change in PAI-1, relative to the +TGF β control, for all trials under each experimental condition. The analysis revealed a statistically significant difference in PAI-1 levels among the experimental conditions. Furthermore, the analysis revealed a statistically significant difference between band density of each experimental condition and the positive TGF β control. Specifically, all antibody treated samples exhibited PAI-1 bands of lower density than the positive control. There was no significant difference identified between the negative control and the -TGF β +mAbs samples, as expected. Furthermore, samples activated by TGF β and treated with mAbs exhibited no significant difference in band density from the negative control. Therefore, activated cell samples treated by TGF β appear to

show evenly reduced normalized PAI-1 band density in comparison to the +TGF β control.

Having analyzed Immunoblot data, we transitioned towards a complementary analytical approach: the enzyme-linked immunosorbent assay (ELISA). While Immunoblotting offered valuable qualitative information regarding changes in PAI-1 levels between experimental conditions, ELISA provides a more

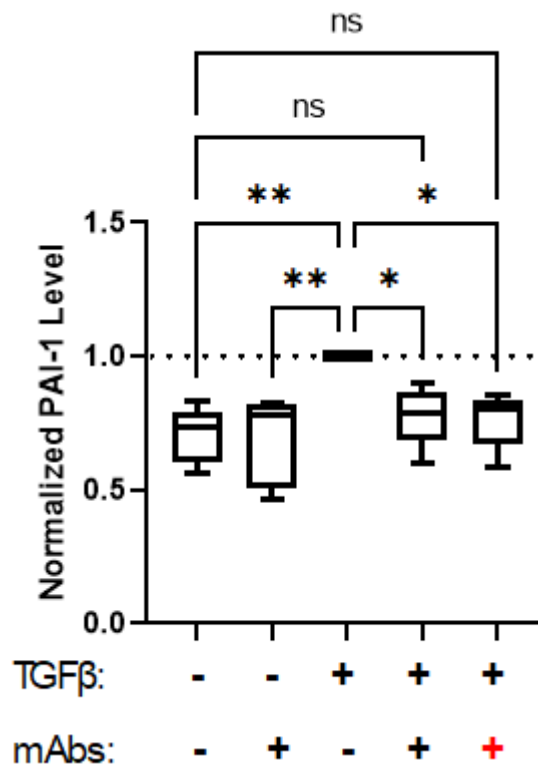


Figure 6: Densitometry of PAI-1 Immunoblot Data Showing Relative Band Density. Immunoblot images were analyzed using ImageJ v1.54h, and the relative band densities were measured and normalized with GAPDH. Concentrations of mAbs: (50 μ g/mL (+) and 100 μ g/mL (+)). Statistical analysis was performed using GraphPad Prism 9.0.0 with a one-way ANOVA test. The graph displays the fold difference between the density of the +TGF β bands and each individual treatment group. Single asterisk represents p<0.05. Double asterisk represents p<0.01. Overall p-value was 0.002, indicating a statistical significance (p<0.05). Individual adjusted p-values for comparisons were calculated utilizing a Dunnet's Multiple Comparisons Test: +TGF β vs. -TGF β (0.0028), +TGF β vs. -TGF β +50mAbs (0.0016), +TGF β vs. +TGF β +50mAbs (0.0316), and +TGF β vs. +TGF β +100mAbs (0.0221), all indicating statistical significance. Number of Samples: n=5.

quantitative assessment of PAI-1 levels. Furthermore, the utilization of ELISA would allow for secondary confirmation of the Immunoblot results, which improves the validity of the data. CM from all 9 cell trials, were used for the ELISA procedure. By analyzing the same set of cell samples using both techniques, potential discrepancies or variations arising from sample heterogeneity or experimental artifacts were minimized, enhancing the reliability and robustness of the experimental findings. Consequently, the utilization of matched cell samples for Immunoblot and ELISA analyses ensured allowed for corroboration using different methods of assessment of PAI-1 levels, allowing for a more comprehensive understanding of the experimental outcomes. The CM samples were incubated on pre-coated ELISA plates and the ELISA was performed as to manufacturers specifications for the Molecular Innovations kit and the R&D Systems kit.

In contrast to Immunoblot, in which samples are denatured by 95°C/SDS treatment, ELISA samples are non-denatured. This means that antibody binding to PAI-1 in CM could affect the results of the ELISA and thus it was hypothesized that the antibodies used for treatment, MA-33H1F7 and MA-8H9D4, may result in reduction of detection of PAI-1 in the CM. In order to determine the validity of this hypothesis, an experiment was conducted to determine if the mAbs had any effect on the ability of the ELISA to detect the PAI-1 in the CM samples. Each ELISA procedure involves the usage of a standard curve, which is developed from pre-coated ELISA wells containing known concentrations of PAI-1, provided by the manufacturer. When the ELISA is done, the spectrophotometer provides

absorbance readings. The absorbance values for wells containing the standard concentrations of PAI-1 are then compared to the known PAI-1 concentrations, allowing for the creation of the standard curve, Absorbance/ng/mL PAI-1. The standard curve is then used to determine the concentration of the unknown samples. In order to determine if the mAbs were interfering with the detection of PAI-1 in the ELISA, two curves were made for each ELISA experiment. The first would be the control curve, made from wells with just the known concentrations of PAI-1. The second curve would be the antibody adjusted curve. The adjusted curve would be derived from wells with the same known concentrations of PAI-1, but with the addition of 50µg/mL each of MA-33H1F7 and MA-8H9D4. In order to compare both curves, the expected concentration of PAI-1 was graphed against the absorbance reading obtained through the ELISA, which would reflect the detection of PAI-1 in the wells, as seen in Figure 7.

Upon analysis of the standard curve data, it became clear that the presence of mAbs exerted a significant influence on the ELISA assay's detection mechanism. Specifically, the adjusted curve, made from samples containing mAbs, exhibited a substantial reduction in signal intensity compared to control

MA-33H1F7 and MA-8H9D4 Interference of PAI-1 Detection

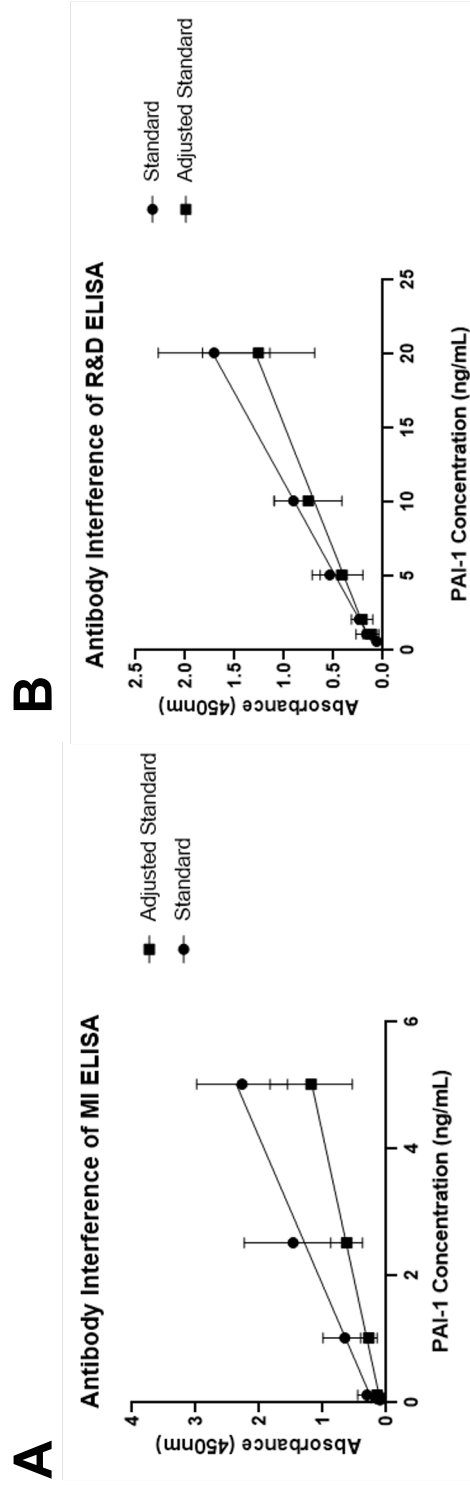


Figure 7: ELISA Standard Curves. Molecular Innovations ELISA (panel A) and R&D Systems ELISA (panel B). Standard curves were generated in duplicates following the respective kit protocols by pipetting the provided standards into designated wells in duplicate. Antibody-adjusted standard curves were created by pipetting duplicate standards into adjacent wells and adding 50 $\mu\text{g/mL}$ of each antibody (MA-33H1F7 and MA-8H9D4) to the wells. The slopes of the MI standard is 0.429, and the slope of the MI adjusted standard is 0.216. The slope of the R&D standard is 0.082, and the slope of the R&D adjusted standard is 0.059; of the. Number of Experimental Repeats: $n = 3$.

samples devoid of antibody treatment. This reduction in signal intensity resulted in a reduction of detected concentrations of about 40% to 60% as seen in Figure 7, and was found to be lower in the R&D systems kit, around 30%. Therefore, all subsequent measurements were performed by the R&D kit.

By incorporating the appropriate corrections based on the observed reduction in signal intensity, we were able to accurately quantify PAI-1 concentrations in the presence of antibody treatment, ensuring the validity of the ELISA data. The CM samples for trials 1-9 were measured for PAI-1 levels using the R&D kit and values for PAI-1 concentration were calculated for both the standard curve and the antibody adjusted standard curve. Each sample was plated in duplicate, and each cell trial had at least 2 individual ELISA tests performed. Average values for PAI-1 level in the CM were calculated using both mAbs adjusted standard curve and the standard curve and can be seen in Figure 8.

Figure 8A reflects the ELISA data for PAI-1 in the CM of all cell trials without any adjustment. The PAI-1 concentrations were calculated directly from the absorbance values obtained and the unadjusted standard curve, which was measured alongside the CM samples. This standard curve does not account for the antibody interference observed. Therefore, Figure 8A reflects the ELISA data as found under standard kit procedure.

In order to account for the antibody standard curve, each concentration for samples treated with mAbs was calculated using an antibody standard curve, as seen in Figure 7. Calculation was performed by taking the absorbance value for

each well containing mAbs, subtracting the y-intercept of the antibody adjusted curve from the absorbance, and dividing by the slope of the adjusted curve.

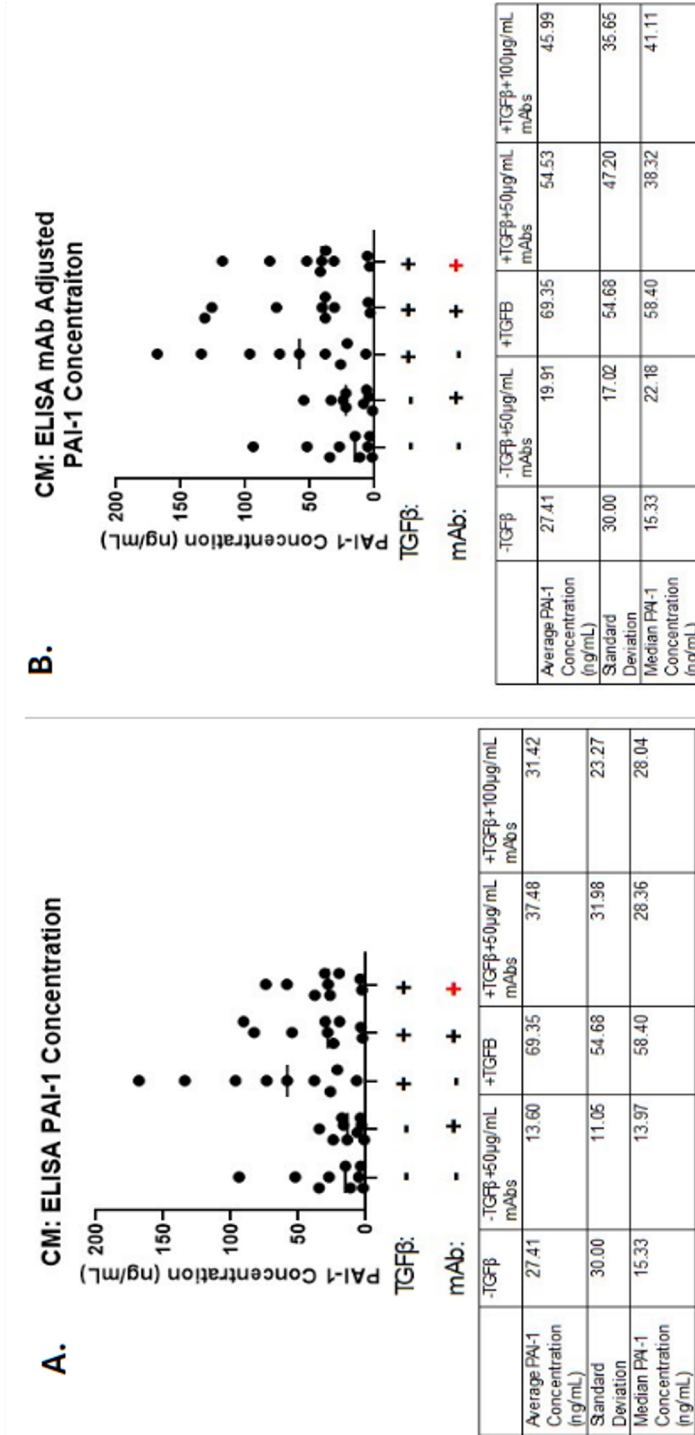


Figure 8: PAI-1 ELISA Data from the R&D Systems Kit. Panel A: Data representing PAI-1 levels under different treatment conditions. Data was obtained using the PAI-1/Serpine kit. Absorbance values were measured at 450nm using a spectrophotometer and concentrations were calculated based on the standard curve following kit instructions. The graph depicts PAI-1 concentration levels across all 9 trials with the average indicated by a horizontal bar in the graphs and statistical values in the table below the graphs. Analysis was performed utilizing GraphPad Prism version 9.0.0. Panel B: Data recalculated using antibody-adjusted standard curves. Data was obtained using the R&D Systems PAI-1/Serpine kit. Antibody-treated wells were adjusted based on the antibody standard curve to compensate for potential antibody interference. The graph depicts PAI-1 concentration levels across all 9 trials, average per trial and experimental condition.

Each ELISA measurement required a separate curve, and therefore samples were all adjusted based on the mAbs treated standard curve run with the samples. Figure 8B reflects the adjusted PAI-1 concentration data. The adjusted values for 8B reflect the average concentrations for each condition in each cell trial across all ELISA tests performed. Each cell trial was tested at least twice using the R&D kit and each adjusted curve was used only for its respective ELISA test.

Figure 8 overall reflects that recalculation of PAI-1 concentration using the antibody standard curve results in an increase in the concentration of PAI-1 detected in CM samples treated with mAbs. There is a noticeable increase in PAI-1 concentration upon adjustment with the antibody standard curves, compared to values seen in 8A. This is reflective of the antibody interference observed in Figure 7, and the adjustment of the data allows for more accurate analysis of the effects of the antibody treatment on PAI-1 expression. The average PAI-1 concentration in samples treated with mAbs is higher in Figure 8B than figure 8A, indicating that adjusting for antibody interference of detection resulted in higher PAI-1 values, which is as expected when accounting for antibody interference. Notably, the values in Figure 8B in mAbs treated lanes are, on average, 31% higher than values seen in Figure 8A for the same conditions. This is reflective of the antibody interference of PAI-1 detection for the ELISA, as the difference in slopes between the standard curve and the antibody standard curve, seen in Figure 7B, is approximately 28%.

Table 1: Table of PAI-1 Concentrations from Conditioned Media.
Adjusted PAI-1 concentration values (ng/ml) obtained through ELISA procedure of CM samples of cell trials 1-9. Values shown in bold indicate concentrations obtained through the antibody adjusted curve.

Trial #	-TGF β	+TGF β	+TGF β +50mabs	+TGF β +100mabs	-TGF β +50mabs
1	15.33	38.25	31.17	31.65	22.18
2	2.04	58.40	38.32	42.13	6.43
3	11.56	21.33	3.58	3.84	1.78
4	5.36	6.90	5.10	5.70	4.66
5	3.87	73.54	40.76	37.74	8.61
6	27.39	26.40	38.17	41.11	22.34
7	34.69	96.70	76.05	52.56	24.61
8	52.45	134.27	126.09	81.3	33.77
9	94.04	168.33	131.56	117.84	54.85

Table 1 reflects the PAI-1 concentrations of condition media samples taken from cell trials 1-9. As seen in the table, when cells are treated with both mAbs and TGF β , the concentration of PAI-1 in the CM decreases, compared to cells treated with only TGF β . This indicates that treatment of cells with mAbs resulted in a reduction in PAI-1 levels in the CM.

ELISA: Changes in PAI-1 Levels in Response to Antibody Treatment

Upon reviewing the data, two cell trials (4 and 6) were removed from the data set as the negative TGF β control demonstrated no significant difference in level of PAI-1 from the positive TGF β control, as seen in Table 1. Furthermore, trials 1, 2, 7, 8, and 9, which had been identified by the Immunoblot as having the expected

PAI-1 bands for the control samples, recapitulate what is expected from published data. These trials all possess +TGFβ controls which have a significantly higher level of PAI-1 than the negative control. Trials 3 and 5 demonstrated significantly higher levels of PAI-1 in the positive TGFβ control, compared to the negative control. This was not apparent in the Immunoblot of these trials and therefore, while the Immunoblot analysis excludes these trials, the ELISA data analysis will include trials 3 and 5. Therefore, cell trials 1, 2, 3, 5, 7, 8, and 9 are the primary focus of the ELISA analysis.

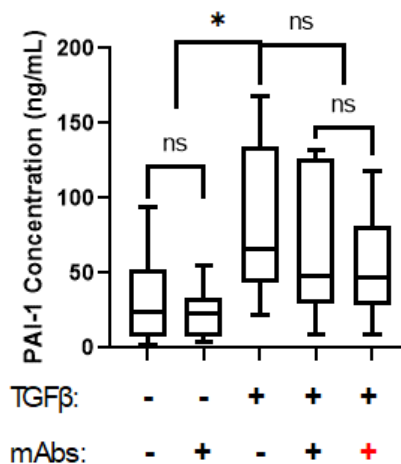


Figure 9: ELISA data Shows a Reduction in PAI-1 Levels in mAbs Treated Sample.

Antibody-treated wells were adjusted based on the antibody standard curve to compensate for potential antibody interference. The graph depicts PAI-1 concentration levels across various experimental conditions, including treatment with TGFβ and different concentrations of antibodies (50μg/mL (+) and 100μg/mL (+)). analysis using one-way ANOVA, performed using GraphPad Prism version 9.0.0. Individual adjusted p-values for comparisons were calculated utilizing a Dunnet's Multiple Comparisons Test. There are significant differences between certain conditions: -TGFβ vs. +TGFβ ($p = 0.047$), -TGFβ+50mAbs vs. +TGFβ ($p = 0.0148$). There were no statistically significant differences observed between +TGFβ vs. +TGFβ+50mAbs ($p = 0.908$), and +TGFβ vs. +TGFβ+100mAbs ($p = 0.537$). There was a significant difference for +TGFβ+50mAbs vs. +TGFβ+100mAbs ($p = 0.560$). The analysis is based on a sample size of $n = 7$.

ELISA data analysis revealed changes in PAI-1 levels upon antibody treatment (Figure 9). The analysis showed a slight decrease in PAI-1 levels in the antibody-treated, TGF β -activated samples compared to the TGF β control (Figure 9). Statistical analysis indicated significant differences between the -TGF β and +TGF β conditions and -TGF β +50 μ g/mL mAbs and +TGF β conditions. However, there was no statistically significant difference between the TGF β -activated antibody-treated conditions (+TGF β +50 μ g/mL mAbs and +TGF β +100 μ g/mL mAb) and the TGF β control.

Relationship Between Immunoblot Data and ELISA Data

Relating ELISA and Immunoblot data in terms of percent difference from the positive control (+TGF β) provides complementary results reflecting PAI-1 expression/secretion changes. By expressing the changes in PAI-1 levels as a percentage of a reference condition, the control +TGF β condition, we are able to account for inherent differences in ELISA data and Immunoblot data.

Figure 10 presents the results of both Immunoblot and ELISA analyses, depicting the percent reduction of PAI-1 levels in response to the TGF β and mAbs treatment. The Immunoblot data in Figure 10 reflects the results of cell trials 1, 2, 7, 8 and 9. The ELISA data for samples containing mAbs was calculated using the antibody adjusted curve as explained prior. In Panel A, the Immunoblot data reveal no statistically significant difference in the percent reduction of PAI-1 levels

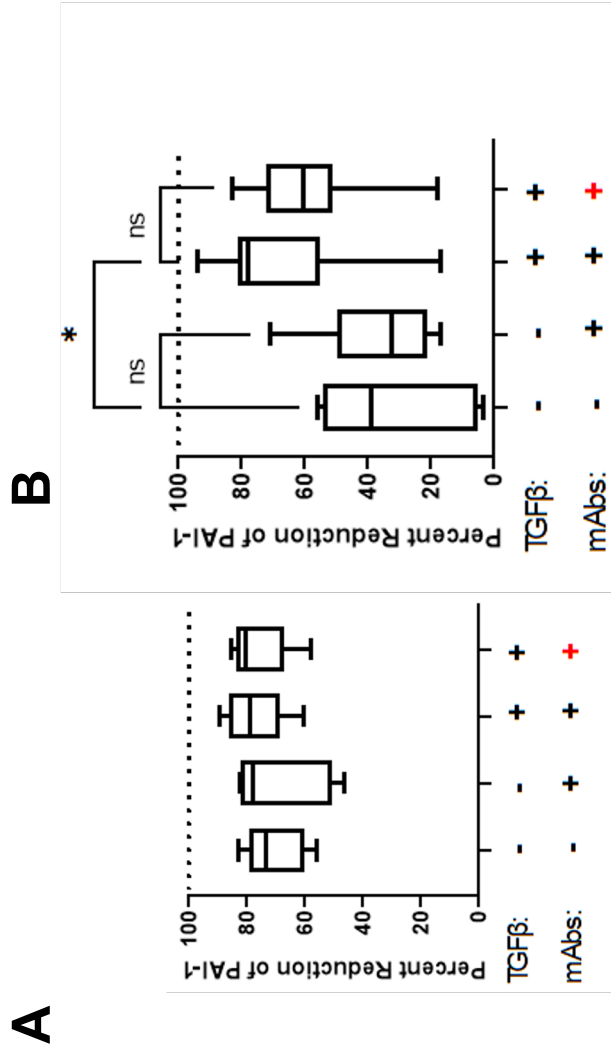


Figure 10: Comparison of PAI-1 levels from Immunoblots and ELISAs. Panel A: Percent reduction of PAI-1 levels from the TGFβ positive control, determined from Immunoblot analysis (n=5). The data were derived by comparing the normalized band densities of each experimental conditioned to those of the +TGFβ control. Concentrations of mAbs: 50μg/mL (+) and 100μg/mL (+). Individual adjusted p-values for comparisons were calculated utilizing a Dunnett's Multiple Comparisons Test. Statistical analysis revealed no statistically significant difference between the percent reduction of PAI-1 levels among samples (p=0.670). Panel B: Percent reduction of PAI-1 levels from the TGFβ positive control, determined from ELISA measurements. Statistical analysis indicated a significant difference (p=0.031) between the +TGFβ+50 μg/mL mAbs treated samples and the -TGFβ control. However, no statistical significance was observed between the +TGFβ+50 μg/mL mAbs and +TGFβ+100 μg/mL mAbs conditions (p=0.915), nor between the -TGFβ+50 μg/mL mAbs and -TGFβ conditions (p=0.996).

among samples ($p=0.670$). This suggests that there was no noticeable change in PAI-1 signal reduction attributable to antibody treatment with Immunoblot detection. Moreover, no significant difference was observed between different experimental conditions, indicating consistent outcomes across all treatment groups. Conversely, Panel B displays the ELISA-derived percent reduction of PAI-1 levels of the same cell trials shown in Panel A, revealing a significant difference ($p=0.031$) between the +TGF β +50 μ g/mL mAbs treated samples and the -TGF β control. This suggests that the decrease in PAI-1 level caused by the mAbs did not bring PAI-1 levels down to the levels observed in the negative control.

Importantly, the ELISA data did not corroborate the trends observed in Figure 4. While 3 samples demonstrated increased PAI-1 band density in lanes containing +TGF β and mAbs, the ELISA data demonstrated a decrease in PAI-1 concentration in these same samples, as seen in Table 1. Cell trial 9, as seen in Figure 3, demonstrates darker PAI-1 bands in activated and mAbs treated sample. Trial 9, as seen in a, shows a reduction in PAI-1 levels for the same sample. Therefore, the ELISA data provides contradictory results to the findings of the Immunoblot for three cell trials, 9, 8, and 7.

Correlating results for the ELISA and Immunoblot analyses served to corroborate the observed trends in measured PAI-1 levels and ensure the reliability of the conclusions. Correlation allows for the evaluation of the degree of agreement between Immunoblot and ELISA results. This assessment helps understand the reliability and consistency between the two methods used, identifying any potential

discrepancies or limitations inherent in each method. Correlation analysis was performed on trials 1, 2, 7, 8, and 9 because the remaining trials displayed ELISA or immunoblot outcomes where no elevation in PAI-1 was observed for the positive control.

The correlation between Immunoblot data and ELISA data was assessed (Figure 11). The percent reduction in PAI-1 level, in comparison to the plus TGF β control, was graphed for all experimental conditions comparing Immunoblot results to ELISA results. The data showed a moderate positive correlation between the ELISA results and the immunoblotting results. Furthermore, the correlation curves show a trend for the data. The data points cluster together more on the x axis, indicating a lower range of variance, and are more spread out along the y axis,

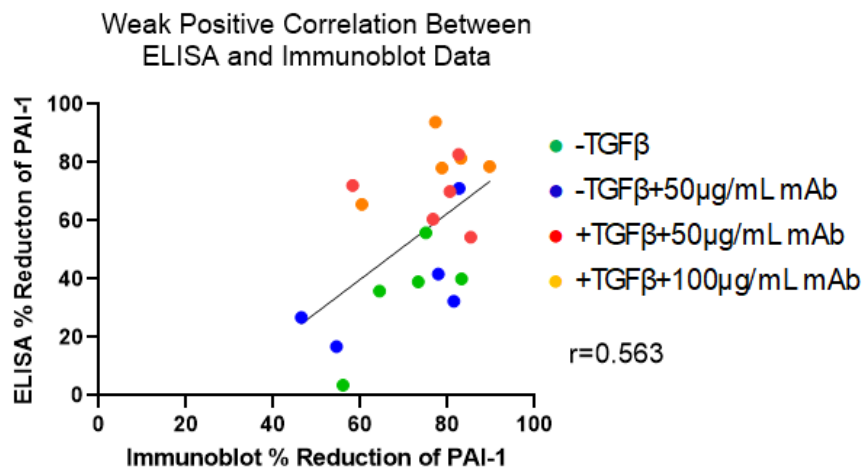


Figure 11: Correlation Plot of PAI-1 Immunoblots Versus ELISAs. Percent reduction in detected PAI-1 from the +TGF β control for the ELISA data (refer to Figure 10B) was graphed against percent reduction in band density from the +TGF β control for the normalized Immunoblot data (refer to Figure 10A). Correlation is for trials 1, 2, 7, 8, and 9. This plot demonstrates the correlation between the two measurement methods, indicating the strength and direction of the relationship. Strong positive correlations is ($r > 0.7$) while a moderate positive correlation is ($r > 0.5$). The correlation was determined utilizing GraphPad Prism and a correlation analysis. The r value obtained from the data revealed a correlation of 0.563, indicating moderate level of agreement between the two methods, immunoblot and ELISA for 5 of the 9 trials.

indicating higher range of variance in x values. Since the y axis is reflective of the ELISA, this indicates that the Immunoblot detected PAI-1 in a closer range than the ELISA, which found the range of PAI-1 levels to be larger than that detected by the immunoblot.

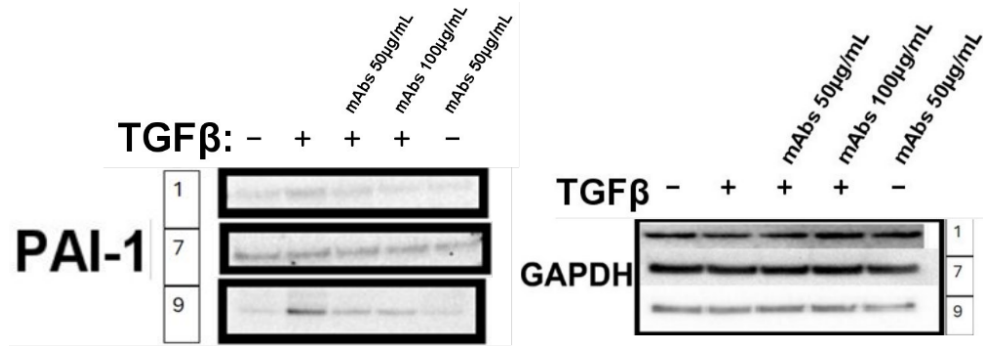
Analysis of PAI-1 in Cell Lysates

Following the analysis of CM from the cell trials, we moved on to the second stage of this study: analysis of PAI-1 in the cell lysates. As PAI-1 is an excreted protein, the levels of PAI-1 within cell lysates are expected to be far lower, and therefore more difficult to detect through the same procedures used for the CM. Furthermore, an immunoblot of cell lysates is expected to contain increased non-specific binding, due to the nature of proteins within the lysate.

Figure 12A shows the results of the immunoblot detecting PAI-1 in the lysate of cell trials 1, 7, and 9. Immunoblot was performed for the cell lysates of other trials as well, however only cell trials 1, 7, and 9 showed a clear band present at 47kDa indicating PAI-1. The other immunoblots had no detectable bands thus could not be evaluated. The faintness of the bands in trials 1, 7, and 9 indicates a lower level of PAI-1 than was observed in the CM. Furthermore, the PAI-1 band for cell lysate immunoblots is thin and appears as a single solid band. This is different than Figure 3, as these trials demonstrated a PAI-1 band which is broad and has a darker area and lighter area.

Furthermore, while the lysate of trial 9 demonstrated a clear increase in PAI-1 in the positive control, the lysates of 7 and 1 did not reflect this. Trial 9's lysate demonstrated a similar trend observed in the Immunoblot band analysis of the CM, a reduction in PAI-1 levels in samples treated with both TGF β and mAbs in comparison to the positive control. While the Immunoblot analysis of lysates reveals high variance and difficulty in band detection, the lysates of trial 9 reflect a reduction in PAI-1 band intensity, indicating a reduction in PAI-1 expression, in the TGF β activated, antibody treated samples. While immunoblot was performed on cell lysate of trials 1-9, only 3 trials yielded visible PAI-1 bands. Furthermore, only one immunoblot displayed a clear increase in PAI-1 band density between the negative control and the positive control. Figure 12B reflects the normalized PAI-1 band densities of the immunoblots of cell lysate trials 1, 7 and 9. In this Figure it a trend of reduction in PAI-1 band density due to mAbs can be observed, as the mAbs treated, TGF β activated lysates appear to have a reduction in PAI-1 levels. Despite visual confirmation of the trend, due to small sample size and low band resolution, no statistically significant differences in band density could be identified. Due to the difficulty of measuring PAI-1 in lysate samples, a secondary method of PAI-1 detection was identified, immunofluorescence.

A.



B.

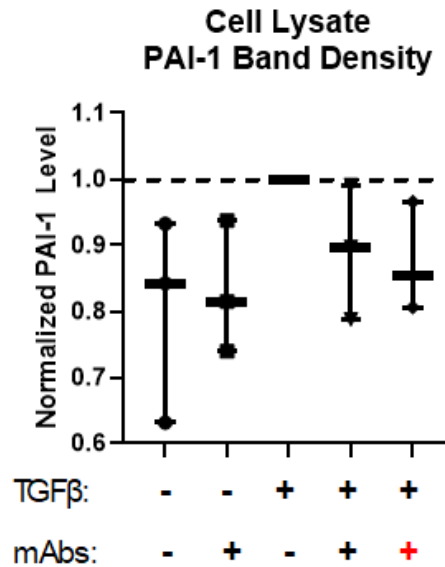


Figure 12: Detection of PAI-1 in Cell Lysates.

Panel A: Cell lysate samples (trials 1, 7, 9) were loaded onto non-reducing gels, separated by electrophoresis, and transferred to PVDF membranes. The membrane of trial 1 was probed for PAI-1 expression using the primary antibody mouse anti-human PAI-1 (C-9) (0.2µg/mL), followed by secondary antibody AffiniPure Donkey Anti-Mouse IgG (0.08µg/mL). The membranes of trials 7 and 9 were probed using the primary antibody rabbit anti-human PAI-1 (0.2µg/mL) followed by secondary antibody goat anti-rabbit IgG (0.8µg/mL). Protein bands were visualized using SuperSignal West Femto Maximum Sensitivity Substrate. GAPDH was used to normalize the data. GAPDH (primary: anti-GAPDH antibody GA1R) was used as control and utilized donkey anti-mouse secondary (0.08µg/mL). Panel B: Cell Lysate Band Density. Band densitometry of measurable cell lysate immunoblots was measured using ImageJ. Bands were normalized using GAPDH and the +TGFβ samples as positive controls. Statistical analysis using one-way ANOVA, performed using GraphPad Prism version 9.0.0. While a reduction in PAI-1 band density due to mAbs was noted, statistical analysis revealed these changes to be statistically insignificant, $p > 0.05$. Number of samples: $n = 3$

Immunofluorescence

Immunofluorescence (IFC) was utilized in order to provide further validation to the ELISA and Immunoblot results. While IFC cannot make determinations of PAI-1 in CM, it can allow for the further validation to the ELISA and Immunoblot results as well as to diversify methodology. The procedure involved fixation, blocking, primary and secondary antibody incubation, and nuclear staining to visualize and quantify the expression of PAI-1 on the cells. Figure 13 reflects images taken following the IFC procedure, with green representing PAI-1 (detected through the GFP channel) and the blue depicting the nucleus (detected through the DAPI channel).

As seen in Figure 13 a reduction in PAI-1 fluorescence intensity was observed in cells treated with both TGF β and mAbs when compared to the +TGF β control. This indicates a reduction in PAI-1 levels on these samples. No statistically significant difference is observed in the fluorescence of samples treated with 50 μ g/mL mAbs or 100 μ g/mL mAbs. A total of 4 sets of IFC trials were conducted, each with a set of conditions identical to those for the Immunoblot and ELISA. Each trial had the following samples: -TGF β , +TGF β , -TGF β +50 μ g/mL mAbs, +TGF β +50 μ g/mL mAbs, and +TGF β +100 μ g/mL mAbs.

Using Gen5 software, a fluorescence emission analysis of each sample was performed, identifying intensity of PAI-1 in each image, and normalized against a DAPI cell count. Figure 14 reflects the relative fluorescence intensity of PAI-1

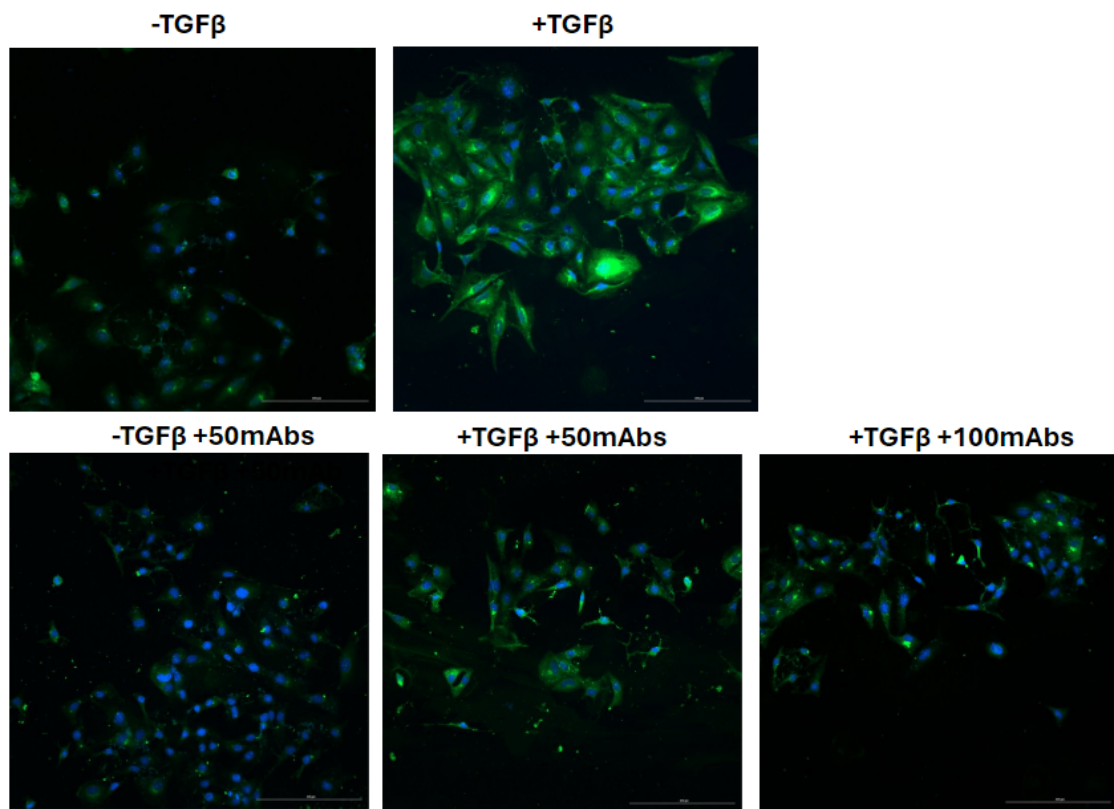


Figure 13: Immunohistochemistry Analysis of PAI-1 Levels in Human Mesothelial Cells. Immunohistochemistry staining was performed on Met5A cells treated with TGF β and mAbs. Cells were subjected to the following treatments: -TGF β , +TGF β , -TGF β +50 μ g/mL mAbs, +TGF β +50 μ g/mL mAbs, and +TGF β +100 μ g/mL mAbs. The primary antibody used for PAI-1 detection were rabbit monoclonal anti-human PAI-1 (0.1 μ g/mL) and the secondary antibody was AlexaFluor 488 Goat anti-rabbit (0.1 μ g/mL). Additionally, nuclear staining was performed using Hoechst 33342 (0.1 μ g/mL). The images were acquired using a Cytation 10 confocal microscope using the GFP (488nm) channel to image PAI-1 and DAPI (405nm) channel for the nuclear stain.

detected from each IFC image. While no statistically significant differences were identified through Gen5 analysis, Figure 14 does show a slight reduction in PAI-1 levels as a result of the antibody treatment on activated cells.

In conclusion, the results presented in Figure 14 indicate that there were no statistically significant changes in fluorescence intensity (reflecting PAI-1 levels) among the different experimental groups based on the statistical analysis. However, upon visual inspection of the IFC images, a notable reduction in PAI-1

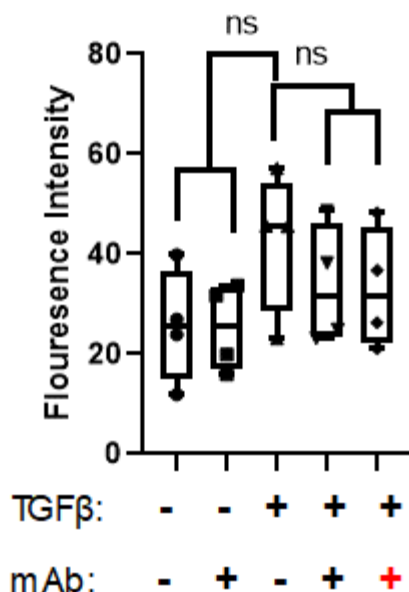


Figure 14: PAI-1 Intensity via Immuno-Fluorescence. IFC staining was performed on Met5A cells treated with TGFβ and mAbs. Cells were subjected to the following treatments: -TGFβ, +TGFβ, -TGFβ+50μg/mL mAbs, +TGFβ+50μg/mL mAbs, and +TGFβ+100μg/mL mAbs. Concentrations of mAb: (50μg/mL (+) and 100μg/mL (+)). Statistical analysis using one-way ANOVA, performed using GraphPad Prism version 9.0.0. Individual adjusted p-values for comparisons were calculated utilizing a Dunnet's Multiple Comparisons Test. No statistically significant differences between conditions were identified. -TGFβ vs. +TGFβ ($p = 0.26$), and -TGFβ+50μg/mL vs. +TGFβ ($p = 0.24$). There were no statistically significant differences observed between +TGFβ vs. +TGFβ+50mAbs ($p= 0.82$), +TGFβ vs. +TGFβ+100mAbs ($p = 0.78$), or +TGFβ+50mAbs vs. +TGFβ+100mAbs ($p = 0.10$). The analysis is based on a sample size of $n = 4$.

levels is observed in the samples treated with both mAbs and TGFβ compared to the TGFβ-activated control group. This visual observation is corroborated by Figure 14 as it also shows a reduction in intensity of fluorescence in the +mAb+TGFβ conditions. This suggests that the antibody treatment may have an inhibitory effect on PAI-1 expression upon TGFβ activation, leading to a decrease in PAI-1 levels. Despite the lack of statistical significance, these findings warrant further investigation into the potential regulatory mechanisms underlying the observed changes in PAI-1 expression. Furthermore, the IFC results validate the

Immunoblot results of the cell lysates of sample 9. In Figure 12, we can see that the PAI-1 bands of trial 9 increase in density for the TGF β control, then decrease in intensity for both mAbs treated samples, which have also been treated with TGF β . This is the same trend observed in the IFC images, indicating that the decrease in PAI-1 observed due to the mAbs may be valid. While IFC cannot provide conclusions for PAI-1 in CM, it does show that the expression of PAI-1 was reduced by the mAbs in activated cell samples. This is directly supporting the observations of the ELISA and Immunoblot analysis and further supports the hypothesis that mAbs may reduce PAI-1 expression in activated mesothelial cells.

IFC procedure was also performed using MA-33H1F7 and MA-8H9D4 individually to treat the Met5A cells. This was done in order to determine if any difference in PAI-1 levels could be observed with only one mAb present. Cells were subjected to the following treatments: -TGF β , +TGF β , +TGF β +50 μ g/mL mAbs, +TGF β +50 μ g/mL MA-33H1F7 and +TGF β +50 μ g/mL MA-8H9D4. IFC procedure was followed as before and the resulting data can be seen in Figure 15.

As seen in Figure 15, IFC of the effect of individual mAbs revealed that MA-8HD94 appeared to result in a reduction in PAI-1 detected. The PAI-1 levels of MA-33H1F7 treated cells appear unchanged. The reduction in PAI-1 levels detected for sample treated with both mAbs appears to exceed the reduction for MA-8H9D4 alone.

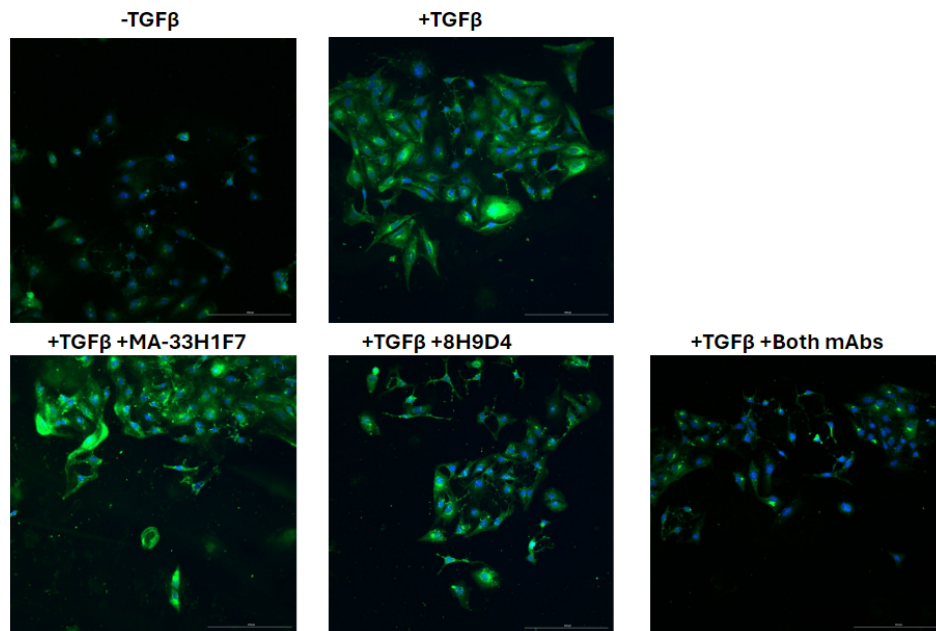


Figure 15: IFC Analysis of PAI-1 in Human Mesothelial Cells.

IFC staining was performed on Met5A cells treated with TGF β and mAbs. Cells were subjected to the following treatments: -TGF β , +TGF β , +TGF β +50 μ g/mL mAbs, +TGF β +50 μ g/mL MA-33H1F7 and +TGF β +50 μ g/mL MA-8H9D4. The primary antibody used for PAI-1 detection were rabbit monoclonal anti-human PAI-1 (0.1 μ g/mL) and the secondary antibody was AlexaFluor 488 Goat anti-rabbit (0.1 μ g/mL). Additionally, nuclear staining was performed using Hoechst 33342 (0.1 μ g/mL). The images were acquired using a Cytation 10 confocal microscope using the GFP channel to image PAI-1 and DAPI for the nuclear stain. PAI-1 levels appear to decrease on cells treated with both mAbs and TGF β . PAI-1 levels appear to decrease with MA-8H9D4 but levels with MA-33H1F7 appear unchanged.

Figure 16 reflects the statistical analysis performed to display IFC data for Figure 15 as normalized relative intensity of PAI-1.

Figure 16 shows a trend of reducing PAI-1 fluorescence intensity with mAbs treatment, However, a statistical analysis revealed no significant changes in PAI-1 fluorescence intensity between the samples. While there was a visual reduction in PAI-1 noted between mAbs treated samples and the positive control,

low sample size and sample variability render any changes in PAI-1 levels statistically insignificant.

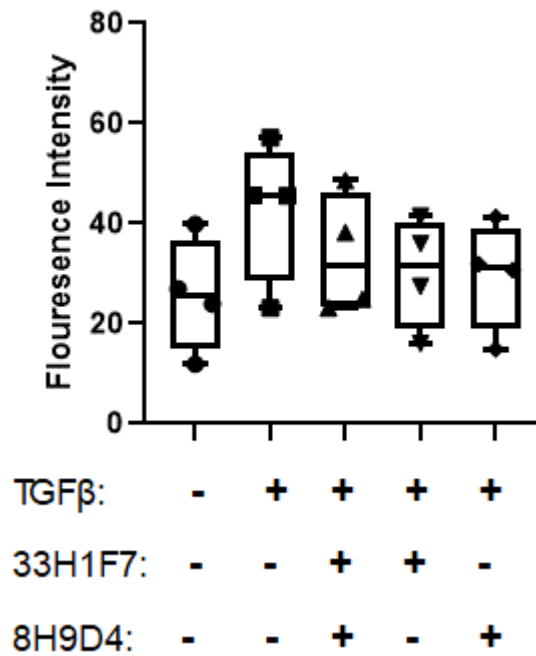


Figure 16: IFC Data for PAI-1 with mAb Treatment. IFC data was obtained and analyzed through Gen5 software. Statistical analysis using one-way ANOVA, performed using GraphPad Prism version 9.0.0. Individual adjusted p-values for comparisons were calculated utilizing a Dunnet's Multiple Comparisons Test. No statistically significant differences between conditions were identified. -TGFB vs. +TGFB ($p = 0.22$), and +TGFB+mAbs vs. +TGFB ($p = 0.76$). There were no statistically significant differences observed between +TGFB vs. +TGFB+33H1F7 ($p = 0.50$), or between +TGFB vs. +TGFB+8H9D4 ($p = 0.46$). Results indicate no statistically significant difference across all samples. The analysis is based on a sample size of $n = 4$.

DISCUSSION

Introduction to the Study

The overexpression of PAI-1 in human empyema serves as the basis of this research. PAI-1 has emerged as a potential therapeutic target due to its implication in empyema as well as various other physiological maladies. Prior studies on PAI-1 in cells, have developed a model to analyze PAI-1 in TGF β activated human pleural mesothelial cells, Met5A [15]. Previous preclinical investigations have also demonstrated that targeting PAI-1 with mAbs can significantly enhance the efficacy of IPFT, leading to a remarkable up to 8-fold increase in treatment efficacy in rabbit models [7].

Despite these promising outcomes, an important knowledge gap persisted regarding the potential effects of mAbs on the expression of PAI-1, as well as other crucial pro-inflammatory and pro-fibrotic markers, within activated human cells. Therefore, our study aimed to bridge this knowledge gap by investigating the impact of mAbs on PAI-1 levels in TGF β activated Met5A cells.

We designed our experimental approach to assess the effects of mAbs on PAI-1 expression using a multi-faceted approach, allowing for the use of multiple different PAI-1 detection techniques. Met5A cells, were subjected to two concentrations of mAbs (50 μ g/mL and 100 μ g/mL), simulating the therapeutic regimen employed in preclinical studies. Subsequently, we evaluated PAI-1 levels in both CM and cell lysate samples using three distinct analytical techniques:

Immunoblot, ELISA, and Immunofluorescence. Through the utilization of these complementary techniques, we were able to demonstrate an effective experimental model in analyzing the cellular effects of PAI-1 targeting using mAbs, as well as identifying a possible impact on PAI-1 expression.

Immunoblot Results Indicate PAI-1 Levels Are Reduced in CM of Activated Cells

Treated With mAbs

This study demonstrates that mAbs, MA 33H1F7 and MA-8H9D4, lead to a reduction in PAI-1 levels in CM of TGF β activated Met5A cells. The reduction of PAI-1 levels due to mAbs was observed in both the Immunoblot results and ELISA results for the CM.

The initial Immunoblot results, as seen in Figures 5 and 3, appear to show a decrease in PAI-1 band intensity in lanes containing CM sample treated with both TGF β and antibodies MA-33H1F7 and MA-8H9D4. The decrease in PAI-1 band intensity due to mAbs, when quantified using densitometry, became less pronounced than visual observations would indicate. This is to be expected as normalization with GAPDH affects the calculation of band density and results in more accurate interpretation of immunoblotting results. Figures 3 and 5 both reflect an apparent decrease in PAI-1 band intensity due to mAbs in TGF β activated samples. This observed trend was found to be independent of the two primary/secondary antibodies utilized. However, Figure 5A demonstrates additional bands

between 150kDa and 120kDa which is only present when the anti-mouse secondary is utilized. Furthermore, the antibodies MA-33H1F7 and MA-8H9D4 are of mouse origin and have molecular weights within 150kDa. Therefore, additional bands at this molecular weight range present in Immunoblots treated with anti-mouse secondary was predicted to be secondary antibody binding non-specifically the mAbs present in the sample. To test this theory mAbs were added to the nuPAGE gel and ran alongside an IgG control antibody, seen in Figure 5B. As seen in the Figure, bands was present between 150kDa and 100kDa which is similar to that observed in Figure 5A. Furthermore, the bands appeared darker in the sample with 100 μ g/mL mAbs. This further supports the theory that the mAbs were detected through non-specific binding with the immunoblotting secondary antibody. Furthermore, the lack of detection in the IgG Lane supports the conclusion that the mAbs account for the bands present at 150kDa.

Uniquely, three cell trials (9, 8 and 7) yielded Immunoblots with PAI-1 bands indicating the opposite effect of mAbs as seen in Figure 3, an increase in PAI-1 band intensity due to antibody targeting of PAI-1. Trial 9, as seen in Figure 3, demonstrated the clearest evidence of the PAI-1 band splitting into two, present at the 52kDa level. This indicates a visualization of the cleaved PAI-1 and latent/active PAI-1. Cleaved PAI-1 has a slightly reduced molecular weight, which will cause it to migrate further down the gel than latent or active PAI-1 [16]. Applying this knowledge to Figure 3 reveals that the presence of cleaved PAI-1 in antibody treated samples is higher than that of the TGF β controls. This is a

confirmation of the success of PAI-1 targeting as the antibodies have done as expected and increased the presence cleaved PAI-1. The lower parts of the PAI-1 bands seen in Figure 3 become clearly darker in lanes containing both mAbs and TGF β . Furthermore, the sample containing just mAbs appeared to display a darker lower PAI-1 band than the -TGF β control, further demonstrating the efficacy of the mAbs.

Additionally, on these 3 gels (trials 9, 2, and 1), bands are seen at the 100kDa range and the 75kDa range, as seen in Figure 4. Figure 4 demonstrates that the TGF β controls both have a band at around 100kda and a band at around 75kDa. The 100kDa band is darker in the +TGF β lane and disappears all together in lanes containing sample treated with antibody. Furthermore, the lower band (75kDa) becomes darker in the antibody treated and TGF β activated samples. This is indicative of the immunoblot having non-specific binding. Specifically, this non-specific binding could likely be a serine protease which interacts with PAI-1. When PAI-1 level is increased due to TGF β treatment, the 100kDa band increases in intensity. When mAbs are present, the 100kDa band vanishes and the lower, 75kDa, band becomes darker. Therefore, Figure 4 reflects crucial evidence of the success of the antibody targeting, as well as an explanation as to the high variance in Immunoblot densitometry data seen in Figure 4. It also suggests that protease activity may have increased due to the inhibition of PAI-1 by the mAbs treatment. The changes in the band pattern at 100kDa and 75kDa are strong indicators that the antibody treatment was successful in eliminating PAI-1 activity. Moreover, the

splitting of the PAI-1 band, splitting into an upper and lower band, further supports the effects of the antibodies. This can be seen in Figure 4 as the lower PAI-1 band increases in density in the presence of mAbs.

The results of immunoblot analysis depicted in Figure 6, which presents the densitometry analysis of the normalized Immunoblot data for trials 1, 2, 7, 8 and 9, shows that mAbs reduce PAI-1 levels in the CM of activated cells. Figure 6 demonstrates that there was a statistically significant reduction in PAI-1 band density when cell samples were treated with both mAbs and TGF β . This is indicative of an inhibitory effect of mAbs on PAI-1 levels in the CM.

ELISA Data Supports The Immunoblot Data

Following the determination of antibody interference of PAI-1 detection of the ELISA, the CM samples of each cell trial were tested for PAI-1 levels using the R&D ELISA kit. Figure 8A reflects the data taken from the ELISA without adjustment with the antibody standard curve. This data was obtained through standard ELISA procedure, using the absorbance values and the standard curve to calculate PAI-1 concentration. In order to adjust the results to account for antibody interference, PAI-1 concentrations for samples containing mAbs were recalculated using the antibody adjusted curve, made for each ELISA measurement. Upon review of published literature, the PAI-1 levels in this study, seen in Figure 8B, were found to fall within the expected range of PAI-1 in CM

sample [15]. While the exact expression of PAI-1 varies between cell lines, the calculated concentrations for this study fall within a 5ng/mL to 150ng/mL range. Furthermore, the ELISA data reflects a strong difference in PAI-1 levels between the positive and negative control. The trials which did not exhibit this difference, 4 and 6, were excluded as the TGF β activation of the cells appears to have failed for these cell trials. Trials 1, 2, 3, 5, 7, 8, and 9 all exhibited a positive control containing significantly more PAI-1 than the negative control upon ELISA analysis. Variations in cellular responses to TGF β can occur due to differences in cell culture conditions, such as cell density, or passage number. Suboptimal cell culture conditions may affect the ability of cells to respond to TGF β stimulation, leading to inconsistent results across samples. Cell passage number again may play a role, as high passage number samples will have reduced viability and different cellular responses than low passage cells. It is likely that a combination of these factors lead to the variance observed in the expression of PAI-1 due to TGF β treatment of the cells.

Importantly, Table 1 reflects that all samples treated with mAbs and TGF β had PAI-1 concentrations which were lower than the +TGF β control. This strongly indicates that mAbs resulted in a lower level of PAI-1 in the CM of activated cells.

In Figure 9, we observe the overall changes in PAI-1 levels in response to antibody treatment as determined by the adjusted ELISA assays. Our analysis revealed a slight decrease in PAI-1 levels in the antibody-treated, TGF β -activated samples compared to the TGF β control. This finding suggests a reduction of PAI-

1 due to mAbs in the activated cells. However, upon closer examination, the high variance observed in the data limits the conclusiveness of this observation. While the apparent decrease in PAI-1 levels is visually discernible, the statistical analysis appears inconclusive.

Specifically, our results indicated significant differences between the -TGF β and +TGF β conditions and the -TGF β +50 μ g/mL mAbs and +TGF β conditions ($P < 0.05$). This indicates that the TGF β treatment was successful, resulting in a significant increase in PAI-1 levels. This is in line with prior research as PAI-1 levels are expected to increase with 10ng/mL TGF β [17]. Upon introducing mAbs treatment in alongside with TGF β activation, the anticipated difference in PAI-1 levels between +TGF β +mAbs and -TGF controls was not observed, suggesting a potential trend toward decreased PAI-1 levels in the CM due to mAbs. Furthermore, the absence of a significant difference between +TGF β +mAbs and +TGF β controls implies that mAbs may indeed reduce PAI-1 levels, potentially restoring them to levels comparable to the negative control. This trend towards decreased PAI-1 expression was also evident in the relative Western blot analysis (Fig 6), reinforcing the notion of mAbs reducing PAI-1 levels.

Figure 9 shows that increasing the mAbs concentration did not result in a further reduction in PAI-1 levels, as expected which indicates that the mAbs concentration is in excess of what is needed to inhibit PAI-1, as no change in PAI-1 level was observed between the lower and higher mAbs concentration.

In order to account for varied PAI-1 levels across cell trials, ELISA data was recalculated as percent difference from the +TGF β control. This means each experimental condition for each trial was compared to the TGF β control for the specific trial. Figure 10B reflects that all mAbs treated TGF β activated sample had lower levels of PAI-1 in the CM, than the TGF β control. This directly supports the theory that mAbs result in a reduction in PAI-1 levels in the CM of activated cells. Furthermore, as seen in 10A, the immunoblot results also showed that samples treated with both mAbs and TGF β all possessed lower levels of PAI-1 than the positive control. Both 10A and 10B reflect that the ELISA data and immunoblot data corroborated the effect of mAbs on PAI-1 levels in the CM.

Figure 11 shows the correlation between PAI-1 reduction, compared to the +TGF β control, measured by Immunoblot and ELISA across the samples. Only Cell trials 1, 2, 7, 8, and 9 were utilized for this correlation, as the others lacked the positive control confirmation. Trials 4 and 6 were excluded due to the lack of positive control conformation observed in the immunoblot, and trials 3 and 5 were excluded for lacking positive control conformation in the ELISA.

Figure 11 also reflects that both ELISA and immunoblot data showed similar trends. The positive correlation, ($r = 0.56$), between the % reduction of PAI-1 in the CM reflects that both methods provided complementary data and both demonstrated that PAI-1 levels are reduced when both TGF β and mAbs are present in sample. The correlation also reveals a key trend for immunoblotting data. All immunoblotting data was clustered closely together on the Y axis, within

a 40% range of reduction of PAI-1 levels. The ELISA data showed a very wide range, almost 100%, which indicates that the ELISA data was much more sensitive to changes in PAI-1 levels. Furthermore, the correlation reveals a weakness of immunoblotting as the detection method was demonstrated to be poor at detecting more minor changes in PAI-1 levels. This is likely due to the nature of immunoblotting and band detection, as variance in density between very light bands is more difficult to quantify. Despite its limitations, immunoblot provided essential information on the efficacy of the mAbs, demonstrating that they did indeed inhibit PAI-1, as well as providing additional information on possible protease interactions with PAI-1.

Immunoblot of Cell Lysates Was Inconclusive

Following thorough analysis of the CM of the cell samples, we moved on to analyze the cell lysates. Figure 12 depicts the result of cell lysate analysis. As stated before, difficulty was found in attempting to visualize the PAI-1 bands present in cell lysates and therefore only 3 lysates could produce analyzable immunoblots. The lysates of trials 1, 7, and 9 can be observed in Figure 12. The lysates of trials 1 and 9 appear to show a decrease in PAI-1 in samples treated with mAbs and TGF β , and the lysate of trial 7 appears to show no change in PAI-1 across samples. The analysis of the bands is limited as trial 1's bands were

found to be very faint, however, trial 9's lysate displayed the clearest trend, of PAI-1 reducing in mAbs treated activated sample.

Studies by have demonstrated that PAI-1 expression increases upon treatment with TGF β in Met5A cells [15]. He also demonstrated that PAI-1 levels are far higher in the CM than in cell lysates. The study by Dr. Shetty identifies that, in contrast to CM, cellular lysates harbor PAI-1 in conjunction with uPAR and uPA within a trimeric complex, susceptible to internalization and subsequent degradation [15]. He goes on to identify difficulties in measuring the PAI-1 levels in cell lysates as samples did not exhibit high variance in PAI-1 due to TGF β treatment, as had been observed in the CM.

This study directly reflects this difficulty as analysis of PAI-1 in cell lysates yielded very few identifiable patterns. Furthermore, as seen in Figure 12 there was high variation in Immunoblot trends between cell trials 1, 7 and 9. Each trial exhibited different PAI-1 band pattern, with 1 having faint hard to quantify bands, 7 containing bands of little variance, and with trial 9 containing a band pattern similar to that identified in the CM, seen in Figure 3. Statistical analysis of immunoblotting of cell lysates did not reveal statistically significant changes in PAI-1 levels across all experimental groups, as seen in Figure 12. This lack of statistical significance is likely tied to the low number of trials, 3, and the low resolution of the PAI-1 bands.

IFC Indicates mAbs Reduce PAI-1 Levels in Cells

In order to corroborate the Immunoblot data for the lysates and provide a tertiary method of data collection, IFC was utilized. For IFC, 4 sets of cell experiments were set up in smaller plates, which would allow for the mounting of the cells. These experiments contained the exact same treatment groups as the initial cell trials seen in Figure 2, which allows for direct comparison of IFC results to the ELISA and Immunoblot data.

Figure 13 reflects the IFC images, taken through confocal microscopy, and shows PAI-1 detection as fluorescence seen in the 5 panels. There is a clear increase in fluorescence, representing PAI-1 detection, when cells are treated with only TGF β . This further corroborates the increased PAI-1 expression due to TGF β which is as expected. Importantly, the intensity of PAI-1 in the mAbs treated, TGF β activated, samples is clearly lower than the +TGF β control. This further demonstrates that mAbs may reduce PAI-1 levels in activated cells. Figure 13 does not show a marked difference in PAI-1 levels between 50 μ g/mL mAbs sample and 100 μ g/mL mAbs samples, further indicating that the amount of mAbs was sufficient at 50 μ g/mL to result in the reduction of PAI-1 as detected by IFC and that an excess of mAbs had no impact on PAI-1 levels. Overall, the IFC images provide strong support for the hypothesis that MA-33H1F7 and MA-8H9D4 result in a reduction in PAI-1 expression/secretion in cells activated by TGF β .

In order to quantify the IFC data, fluorescence analysis was performed with Gen5 software for all samples across all 4 trials. Figure 14 reflects the average fluorescence intensity, reflecting PAI-1 detection, of all 4 trials across each treatment group. Figure 14 identifies PAI-1 detected in the mAbs treated, TGF β activated, samples is lower than the +TGF β control. However, statistical analysis of Figure 14 yielded no statistically significant difference between the +TGF β control and any other treatment group. The lack of statistical significance for the IFC data can likely be attributed to two things. Firstly, there was some variance observed between the fluorescence intensity of the +TGF β treatment group between trials. 2 of the 4, +TGF β , samples displayed less fluorescence intensity than the others. This variability in fluorescence between the same treatment group, could be a result of differences in expression of PAI-1 or a result of procedural errors, such as incomplete washing of secondary or primary antibody. This incomplete washing was observed as artifacts and non-cell bound secondary antibody was observed in several samples. One primary issue found with IFC was the low amount of cells on each slide, which meant that increased washing ran the risk of losing cells on the slide per each wash. In order to combat this, allowing the cells to grow more may help, however too many cells will result in cluttered IFC images which have too many cells, resulting in slides which cannot be accurately analyzed for PAI-1 presence.

Furthermore, it is possible that mAbs may have interfered in IFC detection of PAI-1. IFC, like ELISA, relies on the utilization of detection antibodies, which

must bind to PAI-1 to be detected. The epitope masking, as discussed with the ELISA, could be present within IFC as well. This would result in a reduction in fluorescence intensity in samples with mAbs. Such interference would be greatly reduced as the cells were washed multiple times before permeabilization, however some mAbs may have entered the cell.

Despite this possibility, such an interference effect was not observed by the IFC data. As seen in Figure 14, the -TGF β samples exhibited similar relative fluorescence intensity to the -TGF β +50 μ g/mL samples. The lack of difference in fluorescence intensity between the negative TGF β control and the -TGF β +50 μ g/mL samples indicates that there was no significant interference effect of the mAbs on IFC detection of PAI-1. This indicates that while mAbs may interfere with IFC detection, such interference was not observed in this study.

In order to determine if the mAbs could individually affect PAI-1 levels, an IFC procedure was performed with the following cell treatments: -TGF β , +TGF β , +TGF β +50 μ g/mL mAbs, +TGF β +50 μ g/mL MA-33H1F7 and +TGF β +50 μ g/mL MA-8H9D4. The IFC procedure was carried out the same as before and the results can be seen in Figures 15 and 16. Figure 15 shows IFC images of PAI-1 and cell nucleus overlaid to reflect changes in PAI-1 across treatment group. As seen in the Figure, PAI-1 fluorescence intensity appears to decrease in sample treated with MA-8H9D4 but appears to be unchanged in sample treated with MA-33H1F7. Furthermore, the effect of both mAbs together on PAI-1 appears to be synergistic or additive. The reduction in fluorescence is more apparent in the sample treated

with both mAbs, than the sample treated with just MA-8H9D4. This directly supports established studies which highlight the additive effects of the mAbs [11]. Figure 16 reflects the normalized fluorescence data for the IFC results. While differences in fluorescence intensity were found to be statistically insignificant, likely due to low sample size, the trends observed directly corroborated the images seen in Figure 15. Furthermore, Figure 16 appears to show that both antibodies resulted in a reduction in PAI-1 levels, MA-8H9D4 demonstrated a larger reduction. Despite this, the Figure is unable to validate any synergistic effects of the mAbs as there is no observable difference in relative fluorescence between the +mAbs sample and the +8H9D4 sample.

CM and Cell Analysis Indicates mAbs Reduce PAI-1 Levels

The analysis of PAI-1 both in cells and in CM demonstrates that a reduction in PAI-1 was detected through two independent methodologies, providing support for the effect of mAbs on PAI-1 levels. ELISA and immunoblot data showed that there was a clear reduction in PAI-1 levels in the CM of activated cells treated with mAbs and IFC data demonstrated the same effect directly in the cells. This indicates that mAbs may not only have an inhibitory effect on the secreted levels of PAI-1, but may also result in a reduction in expression of PAI-1, as IFC indicates a reduction in PAI-1 levels due to mAbs treatment.

Possible Mechanisms of Reduction in PAI-1 Due to mAbs

The observed reduction in PAI-1 expression and secretion following antibody treatment, seen in both ELISA and IFC data, raises intriguing questions regarding the underlying mechanisms involved. One possible explanation is that the mAbs, MA-33H1F7 and MA-8H9D4, target specific epitopes on PAI-1, thereby altering its conformation and functionality. Previous studies have demonstrated that mAbs targeting PAI-1 can modulate its activity by inducing conformational changes that affect its interaction with binding partners and cellular receptors [18]. Additionally, the binding of antibodies to PAI-1 may interfere with its stability or promote its degradation, leading to either increased or reduced levels of PAI-1 in the cellular environment [16]. The antibodies may also disrupt the formation of PAI-1 complexes with other proteins or proteases, leading to alterations in its function and turnover [16].

Furthermore, the observed decrease in PAI-1 levels could be attributed to alterations in the endocytic pathway mediated by the low-density lipoprotein receptor-related protein (LRP). LRP plays a crucial role in the internalization and clearance of PAI-1 from the extracellular space through receptor-mediated endocytosis [19]. It has been proposed that PAI-1 forms a complex with LRP when its reactive center loop is inserted, facilitating its recognition and internalization by LRP [20]. Notably, the antibodies targeting PAI-1 induce conformational changes that result in insertion of the reactive center loop, thereby possibly enhancing the

binding affinity of PAI-1 for LRP and facilitating its internalization [20]. There is some support for this theory in the IFC data. In Figure 13 the +TGF β +100 μ g/mL sample has PAI-1 which appears more concentrated in pockets of fluorescence than in the +TGF β +50 μ g/mL sample. This may indicate that the higher antibody concentration is increasing binding to surface receptors, resulting in the spots of high fluorescence intensity observed.

Proteolysis and PAI-1

As seen in Figure 4, proteolytic activity may offer an explanation to the reduction in PAI-1 levels. Figure 4 demonstrates that the mAbs treatment of PAI-1 may result in an increase in protease activity, due to the inhibition of PAI-1 activity. As PAI-1 normally interacts with proteases and inhibits proteolytic activity [21], the mAbs treatment may result in a protection of proteolytic activity, observed in Figure 4. This may then result in the increased degradation of the PAI-1. The protection of proteolytic activity by the mAbs, from PAI-1, would explain the observed decrease in PAI-1 levels in the conditioned media of samples treated with both monoclonal antibodies and TGF β .

Signaling Pathways and mAbs

The activation of inflammatory pathways leads to the induction of transcription factors that bind to the PAI-1 promoter, thereby enhancing PAI-1 gene

expression [16]. The administration of mAbs targeting PAI-1 may modulate this inflammatory response by interfering with PAI-1 activity, potentially affecting downstream inflammatory signaling pathways. Moreover, PAI-1 itself can exert pro-inflammatory effects by promoting the stabilization of extracellular matrix components, facilitating cell migration, and modulating the activity of proteases involved in inflammation [16]. mAbs, while unable to enter the cell on their own, may be able to enter into the cell through internalization of PAI-1 which is bound to mAbs [22]. PAI-1 is regulated by many different signaling molecules such as cytokines, growth factors (TGF β), and hormones [23]. It is possible that the presence of mAbs and presence of increased amount of cleaved PAI-1 results in a signaling feedback loop, resulting in the reduction of PAI-1 expression, due to the already high levels of cleaved PAI-1 present, and due to the antibodies targeting and inhibiting PAI-1.

Conclusions and Future Steps

In summary, our study sheds light on the influence of antibody targeting on PAI-1 in human mesothelial cells. Through a comprehensive analysis employing Immunoblot, ELISA, and IFC techniques, we demonstrated that mAbs targeting and inhibiting PAI-1 can modulate its activity and levels both in the cell and post-secretion. While the statistical significance of the data is marred by high sample variance, this study has provided a strong methodology and procedure

for analysis of the effects of PAI-1 targeting in cells. The observed effects may be mediated by alterations in PAI-1 conformation, endocytic pathways involving receptors like LRP, and interactions with extracellular proteases.

This study provides a strong basis for the analysis of proteolytic activity in relation to PAI-1 targeting. As stated before, this study demonstrates evidence that the targeting of PAI-1 using mAbs may result in the protection of proteolytic activity, which would otherwise be inhibited by PAI-1. This future study could proceed in multiple ways. Firstly, ELISA offers a strong basis for determining activity of a protein. For this, a serine protease could be selected for ELISA which is known to interact with PAI-1. Cells could then undergo TGF β and antibody treatment as performed in this study, with the collection of CM and lysates following incubation. These samples could then be tested for proteolytic activity of multiple proteases, which would shed light on how targeting PAI-1 affects overall proteolytic activity. Furthermore, future studies could determine if PAI-1 is affected on the expression level by the mAbs. The usage of quantitative real-time polymerase chain reaction (qPCR) would allow for the determination of mRNA levels of PAI-1 in relation to antibody treatment. If PAI-1 expression is affected by mAbs, a reduction in mRNA would be detected through the qPCR procedure. For such studies, cell count and consistency are extremely important, as each experimental condition must start with identical conditions in order to definitively determine mRNA changes due to mAbs. The qPCR analysis alongside analysis

of proteolytic activity would not only confirm the reduction in PAI-1 levels due to mAbs treatment, but may also identify the mechanism by which the mAbs result in a reduction in PAI-1 levels.

Additionally, investigations using primary mesothelial cells from rabbit and human sources can provide valuable insights into the translatability of these findings to clinical settings. Moreover, comparative studies between mAbs and alternative targeting agents, such as nanobodies or low molecular weight PAI-1 inhibitors, would help to determine the relative efficacy and safety profiles of these interventions. Such studies would reflect differences in how PAI-1 targeting may affect its activity within cells, its activity post-secretion, and possible changes in expression. By exploring these avenues, we can understand the therapeutic potential of mAbs targeting PAI-1 and their role in mitigating inflammatory and fibrotic processes associated with various diseases such as empyema. By advancing our understanding of PAI-1 biology and its modulation by antibody intervention, we aim to pave the way for the development of targeted therapies for PAI-1-associated pathologies, ultimately improving patient outcomes.

REFERENCES

1. Garvia, V. and M. Paul, *Empyema*, in *StatPearls*. 2024, StatPearls Publishing Copyright © 2024, StatPearls Publishing LLC.: Treasure Island (FL).
2. Chen, Z., et al., *Identification of Microbiome Etiology Associated With Drug Resistance in Pleural Empyema*. *Front Cell Infect Microbiol*, 2021. **11**: p. 637018.
3. Wait, M.A., et al., *Thoracoscopic management of empyema thoracis*. *J Minim Access Surg*, 2007. **3**(4): p. 141-8.
4. Shebl, E. and M. Paul, *Parapneumonic Pleural Effusions and Empyema Thoracis*, in *StatPearls*. 2024, StatPearls Publishing Copyright © 2024, StatPearls Publishing LLC.: Treasure Island (FL).
5. Idell, S. and N.M. Rahman, *Intrapleural Fibrinolytic Therapy for Empyema and Pleural Loculation: Knowns and Unknowns*. *Ann Am Thorac Soc*, 2018. **15**(5): p. 515-517.
6. Chung, C.L., et al., *Proinflammatory cytokines, transforming growth factor-beta1, and fibrinolytic enzymes in loculated and free-flowing pleural exudates*. *Chest*, 2005. **128**(2): p. 690-7.
7. Florova, G., et al., *Targeting of plasminogen activator inhibitor 1 improves fibrinolytic therapy for tetracycline-induced pleural injury in rabbits*. *Am J Respir Cell Mol Biol*, 2015. **52**(4): p. 429-37.
8. Florova, G., et al., *Targeting plasminogen activator inhibitor-1 in tetracycline-induced pleural injury in rabbits*. *Am J Physiol Lung Cell Mol Physiol*, 2018. **314**(1): p. L54-l68.
9. Florova, G., et al., *Targeting the PAI-1 Mechanism with a Small Peptide Increases the Efficacy of Alteplase in a Rabbit Model of Chronic Empyema*. *Pharmaceutics*, 2023. **15**(5).
10. Florova, G., et al., *Precision targeting of the plasminogen activator inhibitor-1 mechanism increases efficacy of fibrinolytic therapy in empyema*. *Physiol Rep*, 2021. **9**(9): p. e14861.
11. Komissarov, A.A., P.J. Declerck, and J.D. Shore, *Mechanisms of conversion of plasminogen activator inhibitor 1 from a suicide inhibitor to a*

- substrate by monoclonal antibodies*. J Biol Chem, 2002. **277**(46): p. 43858-65.
12. Yasar Yildiz, S., et al., *Functional stability of plasminogen activator inhibitor-1*. ScientificWorldJournal, 2014. **2014**: p. 858293.
 13. Masson, P. and S. Lushchekina, *Conformational Stability and Denaturation Processes of Proteins Investigated by Electrophoresis under Extreme Conditions*. Molecules, 2022. **27**(20).
 14. Novoa de Armas, H., et al., *Study of Recombinant Antibody Fragments and PAI-1 Complexes Combining Protein-Protein Docking and Results from Site-Directed Mutagenesis*. Structure, 2007. **15**(9): p. 1105-1116.
 15. Shetty, S., et al., *Post-transcriptional regulation of plasminogen activator inhibitor type-1 expression in human pleural mesothelial cells*. Am J Respir Cell Mol Biol, 2010. **43**(3): p. 358-67.
 16. Sillen, M., et al., *Structural Insight into the Two-Step Mechanism of PAI-1 Inhibition by Small Molecule TM5484*. Int J Mol Sci, 2021. **22**(3).
 17. Cao, H.J., et al., *Transforming growth factor-beta induces plasminogen activator inhibitor type-1 in cultured human orbital fibroblasts*. Invest Ophthalmol Vis Sci, 1995. **36**(7): p. 1411-9.
 18. Sillen, M. and P.J. Declerck, *Targeting PAI-1 in Cardiovascular Disease: Structural Insights Into PAI-1 Functionality and Inhibition*. Front Cardiovasc Med, 2020. **7**: p. 622473.
 19. Cao, C., et al., *Endocytic receptor LRP together with tPA and PAI-1 coordinates Mac-1-dependent macrophage migration*. Embo j, 2006. **25**(9): p. 1860-70.
 20. Herz, J. and D.K. Strickland, *LRP: a multifunctional scavenger and signaling receptor*. J Clin Invest, 2001. **108**(6): p. 779-84.
 21. Bajou, K., et al., *The plasminogen activator inhibitor PAI-1 controls in vivo tumor vascularization by interaction with proteases, not vitronectin. Implications for antiangiogenic strategies*. J Cell Biol, 2001. **152**(4): p. 777-84.
 22. Slastnikova, T.A., et al., *Targeted Intracellular Delivery of Antibodies: The State of the Art*. Front Pharmacol, 2018. **9**: p. 1208.

23. Wyrzykowska, P. and A. Kasza, [*Regulation of PAI-1 expression*]. *Postepy Biochem*, 2009. **55**(1): p. 46-53.

VITA

After graduating from BASIS Peoria, AZ in 2016, Srikar Modukuri entered the University of California Los Angeles, CA as an undergraduate student majoring in Biochemistry. He graduated with a Bachelor of Science in Chemistry in 2020 and In August of 2022 he entered into the Biotechnology graduate program at the University of Texas Health Science Center at Tyler where he performed his thesis work in the lab of Andrey Komissarov.

This thesis was typed by Srikar Modukuri